Lithium isotopes in waters of the tropical volcanic island of Guadeloupe: A proxy of high and low-temperature water-rock interactions

Céline Dessert, Mathieu Dellinger, Clémentine Clergue, Marc F Benedetti, Jérôme Gaillardet

Geochimica et Cosmochimica Acta 417 (2026) 241–255

Contents lists available at ScienceDirect

Geochimica et Cosmochimica Acta

journal homepage: www.elsevier.com/locate/gca

Lithium isotopes in waters of the tropical volcanic island of Guadeloupe: A proxy of high and low-temperature water-rock interactions

Céline Dessert [a,*], Mathieu Dellinger [b], Clémentine Clergue [a], Jérôme Gaillardet [a], Marc F. Benedetti [a]

[a] Université Paris Cité, Institut de physique du globe de Paris, CNRS, F-75005 Paris, France
[b] Université Savoie Mont Blanc, EDYTEM - UMR 5204, 73376 Le Bourget du Lac, France

ARTICLE INFO

Associate Editor: Sambuddha Misra

Keywords:
Lithium isotopes
Tropical rivers
Hydrothermal waters
Critical zone
Andesite weathering

ABSTRACT

This study examines the lithium isotope (δ^7Li) geochemistry of waters flowing through andesitic rocks in order to better constrain the dissolved lithium dynamic in a tropical volcanic island context. We report the first measurements of δ^7Li for eleven of the main rivers in Guadeloupe and four thermal springs on the slopes of La Soufrière volcano. These results have important implications for characterizing the mean riverine flux of lithium coming from the weathering of continental volcanic rocks, understanding the global oceanic budget of lithium, and finally, for interpreting the δ^7Li of past seawater. We have measured a large range of δ^7Li values (3.0–31.6‰) that we explained by different water–rock interaction processes at the scale of this small island. The rivers affected by hydrothermal inputs are the most concentrated and isotopically lighter (δ^7Li from 3.0–12.3‰). This is partly attributed to the leaching and dissolution of clay-rich, hydrothermally-altered rocks which are presumed to have low δ^7Li value and to the discharge from the hot-springs on La Soufrière volcano. The rivers not impacted by hydrothermal inputs are more diluted and isotopically heavier (δ^7Li from 16.0–31.6‰), highlighting two distinct weathering processes in the regolith: the precipitation and dissolution of secondary minerals. In the youngest part of the island, the rivers are characterized by high δ^7Li values, emphasizing that dissolved lithium is mainly controlled by the dissolution of primary andesitic minerals and the incorporation of ^{6}Li into secondary minerals. In the oldest part of the island, the rivers have lower δ^7Li values, which are partly attributed to a low δ^7Li source from the dissolution of secondary minerals in the regolith. We also show a positive correlation between δ^7Li in river waters and the chemical weathering rates (CWR), related to the weatherable primary minerals content in watersheds. We note that this content is linked to rock age, precipitation, regolith type/thickness and geomorphologic parameters such as elevation and slope.

1. Introduction

The surface of the Earth, the Critical Zone, evolves under the coupled action of geology and climate through chemical, physical and biological processes that work together to transform bedrock into secondary minerals, dissolved matter and biota. This complex engine controls the evolution of soils (or regolith in a broader sense), the shape of landscapes, and the riverine transport of dissolved and particulate products from continents to oceans. While it is creating the habitable part of the planet, chemical weathering of Ca–Mg silicate rocks is one of the key geological processes regulating the Earth's global geochemical cycles and the carbon cycle (e.g. Walker et al., 1981; Berner et al., 1983; Raymo and Ruddiman, 1992; Goddéris and François, 1995). The importance of silicate weathering in governing the long-term evolution of the Earth's climate, through the consumption of atmospheric CO_2, has stimulated the development of proxies to constrain past continental weathering.

Over the last decades, the Li isotope ratio has developed as a powerful proxy for silicate weathering reactions (e.g. Huh et al., 1998; 2001; Pogge von Strandmann et al., 2010; Dellinger et al., 2015; Wang et al., 2015; Henchiri et al., 2016). Lithium is mainly hosted in silicate minerals (e.g. Kisakurek et al., 2005; Millot et al., 2010b), and the Li cycle is generally not substantially impacted by biological turnover (Lemarchand et al., 2010; Clergue et al., 2015; Chapela Lara et al., 2022). Moreover, during water–rock interactions, Li isotopes are highly fractionated (Huh et al., 2001). The solution is enriched in the heavy isotope ^{7}Li whereas the light isotope ^{6}Li is preferentially retained by

* Corresponding author.
E-mail address: dessert@ipgp.fr (C. Dessert).

https://doi.org/10.1016/j.gca.2026.01.047
Received 15 April 2025; Accepted 28 January 2026
Available online 3 February 2026

secondary alteration minerals (such as clays). As a result, the dissolved load of both rivers and soil solutions have Li isotope composition (δ^7Li) values higher than the parent rocks (e.g. Huh et al., 1998; Vigier et al., 2009; Millot et al., 2010b; Dellinger et al., 2015; Murphy et al., 2019). No Li isotopes fractionation is observed during mineral dissolution (Pistiner and Henderson, 2003; Wimpenny et al., 2010; Verney-Carron et al., 2011), unlike the precipitation of Li in secondary alteration minerals and the adsorption of Li onto mineral surfaces (Vigier et al., 2008; Millot and Gerard, 2007; Millot et al., 2010a; Li and Liu, 2020; Hindshaw et al., 2019). However, it is still debated whether this fractionation depends on the nature of the secondary mineral involved (Pistiner and Henderson, 2003; Vigier et al., 2008) or is independent of the mineralogy (Dellinger et al., 2015; Li and West, 2014; Hindshaw et al., 2019). Laboratory experiments have also shown that the isotopic fractionation factor inversely correlates with temperature during the formation of Li-bearing secondary minerals (e.g. Williams and Hervig, 2005; Vigier et al., 2008; Millot et al., 2010a; Verney-Carron et al., 2011). Other parameters likely to influence the Li isotopic fractionation are the residence time of minerals (Bouchez et al., 2013; Winnick et al., 2022) and water in the subsurface environment (Liu et al., 2015; Winnick et al., 2022; Zhang et al., 2022a; Pogge von Strandmann et al., 2023).

Misra and Froelich (2012) have shown that marine carbonate δ^7Li has been increasing from 22‰ to 31‰ over the Cenozoic. The interpretation of this trend is complex and the role of change in continental weathering (Misra and Froelich, 2012) vs. high-temperature hydrothermal flux (e.g., Coogan et al., 2017) is debated. In addition, some authors argue that the δ^7Li in rivers increased as a consequence of greater global denudation (e.g. Misra and Froelich, 2012; Li and West, 2014; Rugenstein et al., 2019) whereas others suggested a large change in the Li riverine flux with no change of the isotopic composition (Vigier and Goddéris, 2015). This debate highlights the need to better understand the link between δ^7Li in rivers and the weathering regime.

To that end, we investigated the Li isotopic composition of the rivers of Basse-Terre (Guadeloupe), a tropical volcanic island in the Lesser Antilles arc. This study contributes to a coordinated effort to better constrain new weathering isotopic proxies (Louvat et al., 2011; Clergue et al., 2015; Dessert et al., 2015; Fries et al., 2019; Dessert et al., 2020; Gaspard et al., 2021; Fernandez et al., 2022) and to quantify weathering rates in Guadeloupe at different time-scales (Rad et al., 2006; Sak et al., 2010; Gaillardet et al., 2011; Lloret et al., 2011; Dessert et al., 2015; Guo et al., 2020). Guadeloupe provides the opportunity to study the effects of several parameters on chemical weathering of homogeneous andesitic lithology. First, the regolith composition (with ferralitic soils or Andosols at the surface) results from the combined influence of a north–south age gradient with an east–west pluviometry gradient. The ferralitic northern and central regolith are thicker and more weathered than southern regolith recovered with Andosols. Two previous studies on the highly weathered ferralitic catchment of Quiock Creek (Clergue et al., 2015; Fries et al., 2019) have shown that this small Guadeloupean river exhibits a very low dissolved δ^7Li ratio (~9‰) associated with a transport-limited context with significant secondary mineral dissolution and little contribution from parent rock dissolution to the weathering Li flux. Another important feature of volcanic context is that high-temperature hydrothermal alteration generates different secondary mineral assemblages compared to a low-temperature context (e.g. smectites, zeolites, illites, chlorites). At high temperatures, Li isotope fractionation is limited and the hydrothermal minerals have a δ^7Li ratio close to that of fresh volcanic rock (e.g. Verney-Carron et al., 2015). The presence of such high-temperature neo-formed minerals in altered rocks of the exhumed or active geothermal systems on Basse-Terre Island could influence the Li concentration and δ^7Li ratio of some rivers.

In this study, we report the first measurements of δ^7Li in eleven of the main rivers on Basse-Terre Island and four thermal springs located on the slopes of La Soufrière volcano. We show that the large range of dissolved δ^7Li values (+3 to +31.6‰) is explained by several water–rock interaction processes. Based on these findings, we provide new constraints on Li isotopic fractionation processes that occur in a tropical volcanic context.

2. Study area

The subduction of the North American plate beneath the Caribbean plate generated the Lesser Antilles arc, to which the Guadeloupe archipelago belongs. Basse-Terre Island represents the volcanic part of the Guadeloupe archipelago and covers an area of 950 km^2 (Fig. 1). The island is made up of composite volcanoes of andesitic or basaltic–andesitic composition (e.g. Westercamp, 1988; Boudon et al., 2008).

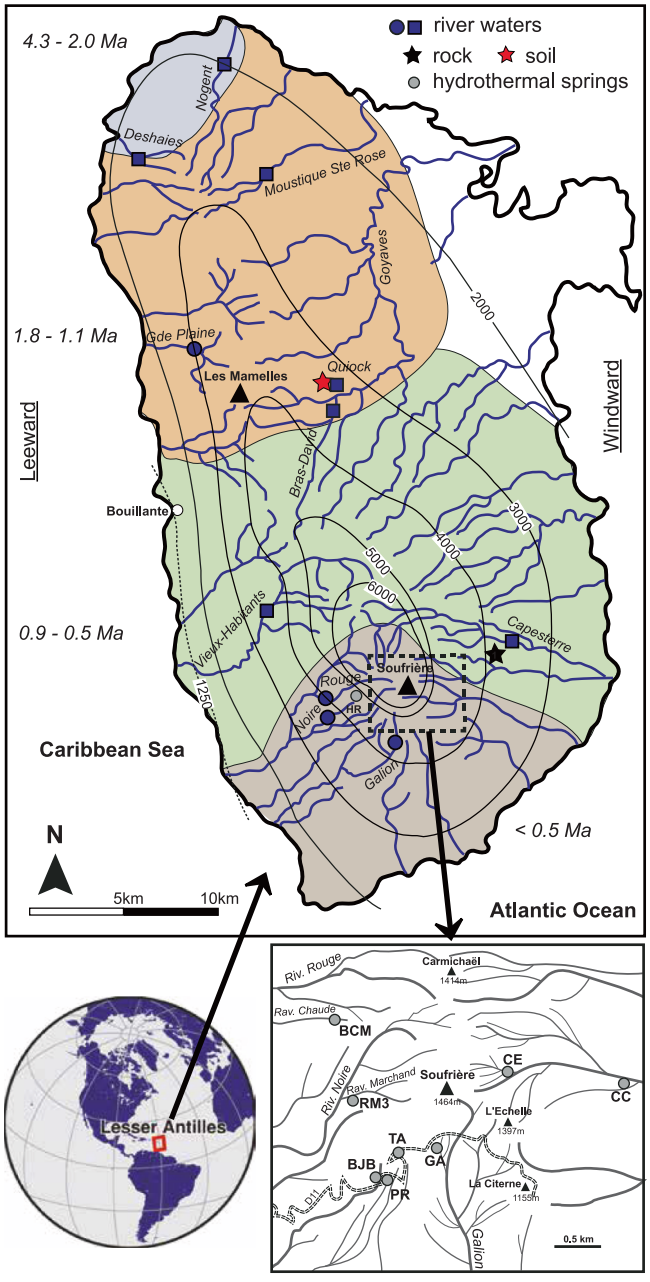

Fig. 1. Sampling locations on Basse-Terre Island. River waters are represented by blue squares, river waters affected by hydrothermal alteration are represented by blue circles, and geothermal spring-water samples are represented by gray circles. The north–south gradient of ages of geological formations is illustrated by the different colored fields (from Samper et al., 2007; 2009; Ricci et al., 2017; Favier et al., 2019). Average annual precipitation is illustrated by the black curves (from 1250 to 6000 mm/yr; Météo France).

The ages of geological formations are reported in Fig. 1 (Samper et al., 2007; 2009; Ricci et al., 2017; Favier et al., 2019). The older, northern part of the island is characterized by Pleistocene-aged volcanism (4.3–2.0 Ma), while the center of the island was formed by volcanic activity 1.8–1.1 Ma ago. The east and the west of the island are composed of Plio-Quaternary (900–550 kyr-old) andesitic formations. Two large volcanic massifs form the youngest part of the island in the south, dating back to 500 ka (Monts Caraïbes massif) and 450 ka (Grande Découverte Complex GDC volcano). La Soufrière de Guadeloupe is the most recent edifice of the GDC volcano, whose volcanic activity began about 9150 years ago (Komorowski et al., 2005; Samper et al., 2009). The last important eruption of this edifice resulted in the construction of the dome of La Soufriere in 1530 CE (Boudon et al., 2008). The hydrothermal system of La Soufrière volcano is very active, with numerous fumaroles and hot springs located around the dome (Fig. 1). Volcanic activity at La Soufrière has been monitored by the Observatoire Volcanologique et Sismologique de Guadeloupe (OVSG-IPGP) since 1950 and the hydrothermal system has been described in detail in previous studies (e.g. Villemant et al., 2014; Tamburello et al., 2019). Thermal springs are concentrated around the base of the dome (mainly in the SW, S and NE sectors) and their distribution is due to the structure of the volcanic edifice and the extensive development of argilic hydrothermal alteration along preferential zones (e.g. Bigot et al., 1994; Villemant et al., 2014; Rosas-Carbajal et al., 2016). The basement of the volcanic structures (caldera and flank collapse craters), to which the recent volcanic activity has been confined, forms preferential zones of shallow groundwater circulation such as the Amic crater structure.

On Basse-Terre Island, fossil high-temperature geothermal systems have also been exhumed and are now exposed to weathering processes. The main hydrothermal surficial manifestations have been identified at (or close to) La Soufrière and Les Mamelles volcanoes, around the bay of Bouillante and in the northern area of Deshaies. In their study on La Soufrière volcano, Salaün et al. (2011) have shown that the hydrothermal alterations observed (smectite + silica polymorphs ± pyrite/jarosite ± gypsum) were typical of alterations caused by low-temperature acid-sulphate fluids (< 150°C). The hydrothermal parageneses observed in the Bouillante area (development of adularia minerals; Patrier et al., 2013; Verati et al., 2014; Navelot et al., 2018) resulted from a high-temperature (i.e. 250–350°C) hydrothermal event. A geothermal power plant was installed in 1986 and expanded in 2005. Another high-temperature mineral assemblage was observed by Favier et al. (2019) in the northern Basal Complex (chlorite, white micas, quartz, actinolite, epidote, biotite and ilmenite, etc…), an exhumed and eroded piece of a deep high-temperature geothermal system.

Basse-Terre Island is characterized by a wet tropical climate with a dry season in winter. The climate is divided into two main seasons and two transitional phases. The dry season runs from January to March with low temperatures and low relative humidity. The wet season runs from July to October with high temperatures and high relative humidity. The two transitional seasons, lasting two and three months respectively, are characterized by variations in temperature and precipitation (https://meteofrance.gp/fr). The mean annual temperature reaches 23°C and humidity is around 75 %. At the Basse-Terre Island scale, a pluviometry gradient is observed depending on topography and influenced by easterly winds. As a result, mean annual precipitation varies between 1200 mm along the west coast and up to 6000 mm/yr at the summit of the Soufriere volcano (Fig. 1; MétéoFrance database https://meteofrance.gp/fr). The abundant precipitation, coupled with steep slopes have generated a dense river network. During the wet season, hurricanes and tropical depressions produce intense individual rainfall events, which play a major role in the erosion of Guadeloupean soils and the transport of weathering products. As an example, the tropical storm Helena, which hit Basse-Terre Island on 24 October 1963, initiated numerous landslides that produced an average denudation of 2800 t/km^2 on the watersheds affected by landslides (Allemand et al., 2014). It has also been shown that floods and extreme floods, which represent around 43 % of the annual water flux, correspond to on average 54 % of the annual dissolved organic carbon flux, 85 % of the annual particulate organic carbon flux, and 20–30 % of the chemical weathering rate (Lloret et al., 2013; Dessert et al., 2015). The transport of boulders (size of 0.5 to 0.75 m) occurs also during extreme floods, for approximately 10 h/yr (Allemand et al., 2023).

Vegetation in the Parc National de Guadeloupe is mainly dominated by tropical rainforest, and by altitude forest at the heads of the watersheds (Van Laere et al., 2016). Previous studies (Clergue et al., 2015; Dessert et al., 2020) emphasized the important role of African dust in fertilizing the tropical rain forest and the impact of atmospheric deposition on stream water. The average deposition mass flux of African dust was estimated to 11.2 g/m^2/yr (Xu-Yang et al., 2022; 2025). The distribution of soils (the top layer of the regolith) in Guadeloupe is related to rock age, precipitation and topography (e.g. Colmet-Daage and Bernard, 1979; Henriet et al., 2008; Buss et al., 2010). The north and northeast edge of Basse-Terre Island are characterized by Vertisols with a high amount of montmorillonite and kaolinite. A large part of the central island has ferralitic soils with iron oxides and different amounts of kaolinite and halloysite. In the south, near the Grande Découverte Complex, Andosols with allophane can be found with various amount of (Al, Fe)–humus complexes, ferrihydrite, gibbsite, poorly crystalline Al hydroxide, depending on the soil evolution stage (Vander Linden et al., 2021). The regolith, grouping soil and the layer of more or less disaggregated andesitic minerals, is separated from the underlying weathered bedrock by the so-called weathering front. The recent study of Pasquet et al. (2022) has combined seismic measurements, petrophysical modeling and geostatistical analysis to characterize the regolith architecture of the Quiock Creek catchment (in the ferralitic central part; Fig. 1). The regolith thickness was estimated between 5 and 15 m, in agreement with previous drilling observations made at the same site (> 12 m; Buss et al., 2010). In a similar tropical volcanic environment in Puerto Rico, Buss et al. (2013) observed regolith thickness down to about 40 m. In Guadeloupe, it can therefore be assumed that the regolith thickness is much greater than 15 m in the old northern part of the island. Conversely, in the young southern part of the island, we observed a regolith thickness around 1 m in the Andosols area of the Capesterre catchment (Fig. 1; Lloret et al., 2016). Schematically, there is a gradient of the pool of weatherable andesitic minerals in regolith, this pool being smaller and deeper in a highly weathered environment. This pool is smaller in the old northern part than in the young southern part of the Basse-Terre Island.

Here, we study eleven of the main rivers on Basse-Terre Island. These rivers define gradients in pluviometry, age and regolith mineralogy/depth. Three rivers were sampled in the north, three rivers in the center, four in the southwest and one in the east (Fig. 1). The main characteristics of these watersheds are presented in Table 1. Four rivers are influenced by hydrothermal alteration around exhumed geothermal systems and around the active La Soufriere volcano (Gaillardet et al., 2011; Rivé et al., 2013; Dessert et al., 2015; Gaspard et al., 2021). Four of these watersheds (Bras-David, Quiock-Creek, Vieux-Habitants and Capesterre) are monitored by the Observatoire de l'Eau et de l'Erosion aux Antilles (ObsERA, part of OZCAR research infrastructure; Gaillardet et al., 2018) dedicated to the study of weathering and erosion processes under tropical climatic conditions. Water samples from four other thermal springs were collected on the slopes of La Soufrière volcano (Fig. 1). Three sampled sources are located at high altitudes (950 m −1150 m) in the Amic crater: Bains-Jaunes (BJB), Galion (GA), and Ravine-Marchand (RM3). The Habitation-Revel spring (HR) is located outside the Amic crater structure, on the eastern flank of the Grande Découverte volcano, 3.5 km east of the dome and at an altitude of around 600 m.

Table 1
Characteristics of studied watershed and sample localization (see Fig. 1).

Site	Latitude	Longitude	Elevation (m)	Watershed area (km^2)	Mean age [a] (My)	Soil type [b]	Runoff (mm/yr)
Northern rivers							
Nogent	N16°20′04.8	W61°44′48.8	560	5.2	> 2.0	Ferralitic soil	780[e]
Moustique Sainte-Rose	N16°17′54.9	W61°42′38.8	114	6.2	2.0	Ferralitic soil	1620[e]
Deshaies	N16°18′05.3	W61°47′29.8	30	4.4	> 2.0	Ferralitic soil	430[e]
Central rivers							
Grande-Plaine	N16°12′33.6	W61°45′39.2	428	10.8	1.5	Ferralitic soil	2000[f]
Bras-David	N16°10′33.6	W61°41′34.8	233	11.0	1.15	Ferralitic soil	2037[d]
Ravine-Quiock	N16°10′40.2	W61°41′39.2	300	0.08	1.5	Ferralitic soil	1130[c]
Southern rivers							
Vieux-Habitants	N16°05′11.8	W61°43′31.3	257	19.1	0.45	Ferralitic soil andNitrisols (smectite, halloysite)	2580[d]
Capesterre	N16°04′18.0	W61°36′34.1	208	16.2	0.55	Andosol	4206[d]
Rivière Rouge	N16°02′51.7	W61°41′09.4	677	2.4	< 0.45	Andosol	4000[f]
Rivière Noire	N16°02′13.7	W61°40′52.1	748	1.2	< 0.45	Andosol	4000[f]
Galion	N16°00′24.0	W61°41′35.2	640	3.0	< 0.45	Andosol	4000[f]

[a] Samper et al., 2007, 2009;Favier et al., 2019.
[b] Colmet-Daage and Bernard, 1979.
[c] Clergue et al., 2015;Guérin et al., 2019.
[d] Dessert et al., 2015.
[e] Lloret et al., 2011.
[f] Gaillardet et al., 2011.

3. Methods

3.1. Sample collection

River water samples were collected manually upstream of anthropogenic (e.g. crops, urban environments) parts of each catchment between 2006 and 2015. Some of these samples have already been studied for their isotopic boron (Louvat et al., 2011) and magnesium composition (Dessert et al., 2015). Capesterre, Bras-David, Vieux-Habitants rivers and Quiock Creek are studied as part of the ObsERA observatory and data are available on the website of the observatory (https://www.ipgp.fr/obsera). Temperature, pH and conductivity were measured in situ. After collection, a non-filtered aliquot of 20 mL was used for measuring alkalinity. The rest of the sample was then filtered at the observatory through a 0.2 μm cellulose acetate membrane filter and stored in polypropylene bottles. A non-acidified aliquot was set apart for anion quantification and another aliquot was acidified with 2 % HNO_3 for cation and trace analyses. Then, samples for Li isotopic measurement were stored in polypropylene bottles previously washed with distilled HNO_3 0.5 N and acidified with 2 % HNO_3.

The water from the four thermal springs was collected in November 2011 and April 2014 on the slopes of La Soufrière volcano. Temperature, pH and conductivity were measured on site and samples were filtered in situ through 0.2 μm cellulose acetate membrane filters.

3.2. Analytical method

Alkalinity was determined using an automatic acid-base titration stand (Radiometer TIM840 with Schott probe). Base cations were measured with an ICP-AES Thermofisher iCap 6200 series at the Institut de Physique du Globe de Paris (IPGP). The detection limits for Na and K were around 10 ppb and around 2 ppb for Mg and Ca. Anions were measured with a Dionex DX 120 chromatography at the IPGP (river samples) and at the OVSG/IPGP (spring samples). The detection limits were around 5 ppb for SO_4 and Cl. Dissolved Li concentrations were measured using a HR-ICP-MS Element II ThermoScientific at IPGP. The limit of quantification for Li was estimated to be 20 ppt and the accuracy was controlled by repeated measurements of SLRS-5 with an external reproducibility of 3 %.

Before the column purification step, water samples were evaporated to dryness and then refluxed with concentrated HNO_3 at 100-120°C to remove the organic matter. As ~20 ng of Li is necessary for measurement with the MC ICP-MS, the volume of water to evaporate varied between 1.2 mL (for the most concentrated hydrothermal spring) to 125 mL (for the least concentrated river). The dry residues were solubilized in 1 mL of HCl 0.2 N before being loaded onto the columns. Li purification was achieved using a cation exchange column filled with Biorad AG50X-12 resin on HCl 0.2 N media following the protocol detailed in Dellinger et al. (2014).

Li isotopes analyses were performed on the Neptune multicollector ICP-MS (Thermo Scientific) at IPGP using the Apex sample inlet system. Details on the analytical procedure are available in Clergue et al. (2015). The δ^7Li is calculated relative to the L-SVEC standard (Flesch et al., 1973) as follows:

$$\delta^7 Li = \left(\frac{\left(\frac{7Li}{6Li}\right) sample}{\left(\frac{7Li}{6Li}\right) L-SVEC} - 1 \right) \times 1000 \quad (1)$$

The external reproducibility, based on repeated measurements of standards is below 0.5‰. The δ^7Li of the NASS-5 seawater standard was measured at +30.73±0.35‰ (2σ; n =9 separations and measurements).

3.3. Source partitioning of major dissolved elements and lithium

The concentration of Li^+, Na^+, K^+, Mg^{2+}, Ca^{2+}, SO_4^{2-}, SiO_2 (Table 2) depends on four different sources: atmospheric input ($[X]_{atm}$), low-temperature dissolution of andesite rocks ($[X]_{LTwea}$), dissolution of clay-rich, hydrothermally-altered rocks ($[X]_{HI\text{-}rock}$) and the discharge of thermal springs ($[X]_{spring}$):

$$[X]_{diss} = [X]_{atm} + [X]_{LTwea} + [X]_{HI-rock} + [X]_{spring} \quad (2)$$

With $[X]_{atm}$, $[X]_{LTwea}$, $[X]_{HI\text{-}rock}$ and $[X]_{spring}$ the dissolved ions concentration in the river water derived from each source (see Table 3 and Table A.1. for calculation results for each element).

For NI rivers, there are no input from thermal springs ($[X]_{spring} = 0$) and from hydrothermally altered rocks ($[X]_{HI\text{-}rock} = 0$). The atmospheric

Table 2
Chemical and isotopic composition of rivers and thermal springs (location in Fig. 1). Concentrations are expressed in µmol/L and Cat and TDS in mg/L.

Site	Date	T (°C)	C (µS/cm)	pH	Na	K	Mg	Ca	Cl	SO_4	Alc	SiO_2	Li	δ^7Li ‰	Cat	TDS
Northern rivers																
Nogent	23/04/2014	21.8	93	7.7	464	28	80	73	429	49	271*	678	0.109	16.9	17	94
Moustique Sainte-Rose[a]	12/12/2006	22.6		7.3	373	19	84	78	370	43	226	389		16.0	14	69
Moustique Sainte-Rose	23/04/2014	22.6	69	7.4	325	19	63	65	312	48	192*	260	0.070	18.2	12	55
Deshaies	23/04/2014	21.3	116	7.6	600	36	101	94	490	63	410*	855	0.106	18.0	21	121
Central rivers																
Grande-Plaine[a]	04/12/2006	22.6		7.2	474	48	164	229	434	356	274	275	0.027		26	109
Grande-Plaine	23/04/2014	24.6	203	7.2	556	31	208	378	385	476	422*	471	0.137	7.6	34	148
Bras-David[a]	17/05/2010			6.8	222	12	28	50	238	24	130	226		23.2	8	41
Bras-David	23/04/2012	24.2	70	6.1	255	16	64	102	222	24	336	227	0.029	26.4	12	56
Bras-David	05/08/2012	24.2	72	7.2	297	14	64	98	231	23	313	320	0.028	26.4	13	77
Bras-David	20/03/2013	21.6	50	7.4	229	11	41	59	227	21	129	139	0.020	28.0	9	35
Bras-David	21/06/2013	24.0	72		254	14	69	106	216	18	328	290		22.5	12	59
Bras-David	25/06/2013	22.8	74	7.2	296	17	65	104	170	20	162	102		20.5	13	37
Quiock Creek[2]	23/04/2012				184	6	25	11	229	15	37	109	0.042	9.3	5	24
Quiock Creek[2]	21/03/2013	22.6	43	4.8	211	3	32	15	274	13	28	112	0.045	7.9	6	26
Quiock Creek[2]	03/04/2013	22.6	39	4.6	217	5	28	12	249	15	34	112	0.038	8.3	6	25
Quiock Creek[2]	25/06/2013	24.2	38		185	5	27	11	246	13	39	130		8.0	6	26
Quiock Creek[3]	21/10/2015	24.7	48	5.3	262	5	28	13	326	10	7	197	0.058	9.0	7	32
Quiock Creek[3]	25/10/2015	24.3	35	4.9	201	5	22	11	226	18	0	131	0.041	7.7	6	23
Quiock Creek[3]	26/10/2015	24.5	42	4.9	245	4	27	11	297	13	0	156	0.051	7.2	7	28
Southern rivers																
Vieux-Habitants[a]	01/11/2006		78	7.6	266	15	72	142	157	29	453	451		18.9	14	77
Vieux-Habitants[a]	11/07/2007	24.4	81	7.8	283	19	77	142	155	33	529	496	0.033	21.3	15	86
Capesterre[a]	11/07/2007	23.8	66	7.7	245	16	59	118	146	28	431	354		31.6	12	68
Capesterre[a]	07/12/2010				115	9	14	33	84	13	181	152	0.014	29.5	5	29
Rivière Rouge	31/10/2012	20.9	178	3.7	288	22	109	400	141	786	0	679	0.138	3.0	26	147
Rivière Rouge	22/04/2014	19.3	69	5.2	171	16	44	125	121	187	30*	271	0.054	4.0	11	51
Rivière Noire	22/04/2014	19.9	172	7.4	397	50	172	362	290	341	543*	506	0.222	12.4	30	136
Galion	22/03/2013			5.6	446	48	299	601	794	725	51		0.289	6.8	43	
Galion	22/04/2014	20.2	103	7.4	268	23	101	199	266	182	261*	280	0.105	9.4	17	77
Thermal springs																
BJB	11/04/2014	29.2	709	5.1	1318	123	766	1984	1106	2803	140		1.776	8.7	133	
GA	11/04/2014	46.9	2080	4.9	2592	474	2767	7064	9976	7074	572		1.169	13.0	428	
HR	01/04/2014	32.2	279	6.6	1112	89	212	520	232	210	1834		2.450	8.3	55	
RM3	07/11/2013	45.1	1911	5.3	2016	406	1649	3870	3516	4660	1247		1.992	12.1	257	

Cat: cationic dissolved load (Na + K + Ca + Mg); TDS: total dissolved load (Cat + HCO_3 + Cl + SO_4 + SiO_2).
*: estimated from charge balance.
[a] : Dessert et al., 2015; [2]: Clergue et al., 2015; [3]:Fries et al., 2019.

Table 3
Mean source partitioning of Lithium and TDS (see Table A.1. for other chemical species).

Site	Li atm	Li LT-wea	Li HI-rock	Li spring	TDS atm	TDS LT-wea	TDS HI-rock	TDS spring
Northern rivers								
Nogent	23 %	77 %	0 %	0 %	52 %	48 %	0 %	0 %
Moustique Sainte-Rose	26 %	74 %	0 %	0 %	61 %	39 %	0 %	0 %
Deshaies	27 %	73 %	0 %	0 %	51 %	49 %	0 %	0 %
Central rivers								
Grande-Plaine	16 %	28 %	55 %	0 %	37 %	16 %	47 %	0 %
Bras-David	53 %	47 %	0 %	0 %	60 %	40 %	0 %	0 %
Quiock Creek	34 %	66 %	0 %	0 %	67 %	33 %	0 %	0 %
Southern rivers								
Vieux-Habitants	27 %	73 %	0 %	0 %	51 %	49 %	0 %	0 %
Capesterre	35 %	65 %	0 %	0 %	56 %	44 %	0 %	0 %
Rivière Rouge	9 %	22 %	69 %	0 %	11 %	21 %	68 %	0 %
Rivière Noire	3 %	8 %	45 %	44 %	31 %	16 %	13 %	41 %
Galion	5 %	11 %	62 %	22 %	32 %	27 %	11 %	29 %

SiO_2 input is negligible and $[SiO_2]_{atm} = 0$ and the elemental mass-balance (X = Li^+, Na^+, K^+, Mg^{2+}, Ca^{2+}, SO_4^{2-}) is:

$$[X]_{NIriv} = [X]_{atm} + [X]_{LTwea} \quad (3)$$

For quantifying the atmospheric input, we can use Cl^- in the dissolved load. In NI rivers, all of the Cl^- in the dissolved load has an atmospheric origin:

$$[Cl^-]_{NIriv} = [Cl^-]_{atm} \quad (4)$$

Lloret et al. (2011) estimated that the concentration of atmospheric Cl^- in rivers varied between 200 µmol/L in the southern part and 800 µmol/L for the Deshaies River in the northern part of the island, depending on

the rainwater Cl^- concentration and the evapotranspiration factor. We can thus assume that all the Cl^- content has mainly an atmospheric origin.

The concentration of the dissolved element (X = Li^+, Na^+, K^+, Mg^{2+}, Ca^{2+}, SO_4^{2-}) resulting from atmospheric input is equal to:

$$[X]_{atm} = [Cl^-]_{atm} \times \left(\frac{X}{Cl}\right)_{rain} \quad (5)$$

(the rainwater X/Cl molar ratio is from Clergue et al., 2015; Dessert et al., 2015; Na/Cl = 0.92, Ca/Cl = 0.11, SO_4/Cl = 0.09, Mg/Cl = 0.1, K/Cl = 0.05, Li/Cl = 5.8 10^{-5}).

Hence, the concentration of the dissolved elements resulting from low-temperature weathering in NI rivers is equal to:

$$[X]_{LTwea} = [X]_{NIriv} - [Cl^-]_{atm} \times \left(\frac{X}{Cl}\right)_{rain} \quad (6)$$

And the mixing proportions of the dissolved element X in each source are:

$$\gamma^X_{atm} = \frac{[X]_{atm}}{[X]_{NIriv}} \text{ and } \gamma^X_{LTwea} = \frac{[X]_{LTwea}}{[X]_{NIriv}} \quad (7 \text{ and } 8)$$

This commonly used Cl-based method provides a maximum estimate of atmospheric input contributions, as it assumes that precipitation-derived solutes behave conservatively and are not significantly affected by secondary processes such as clay precipitation or ion-exchange. This assumption is most likely valid during wet periods in humid tropical catchments such as Guadeloupe, when soils are close to saturation and fast hydrological pathways dominate.

In HI rivers, two supplementary inputs may influence the riverine dissolved load: the leaching and dissolution of clay-rich, hydrothermally-altered rocks ($[X]_{HI\text{-}rock}$) and the discharge of thermal springs ($[X]_{spring}$). Two rivers (Rivière Galion and Rivière Noire) have Cl^- contents exceeding $[Cl^-]_{atm}$ (as estimated from nearby NI rivers; 120 µmol/L), which suggests that they are significantly influenced by the discharge from thermal springs on La Soufrière volcano:

$$[Cl^-]_{HIriv} = [Cl^-]_{atm} + [Cl^-]_{spring} \quad (9)$$

The concentration of the dissolved elements (X = Li^+, Na^+, K^+, Mg^{2+}, Ca^{2+}, SO_4^{2-}, SiO_2) resulting from the discharge of thermal springs is equal to:

$$[X]_{spring} = [Cl^-]_{spring} \times \left(\frac{X}{Cl}\right)_{spring} \quad (10)$$

Making it possible to calculate the proportion of each element ($\gamma^X_{spring} = [X]_{spring}/[X]_{riv}$) derived from thermal springs. We use the X/Cl ratio of the springs GA and RM3 to determine respectively the $[X]_{spring}$ for Rivière Galion and Rivière Noire.

All HI rivers are characterized by a high SO_4^{2-} content, mainly resulting from leaching and dissolution of sulfate hydrothermal minerals (Gaillardet et al., 2011) and from thermal springs. The SO_4^{2-} mass-balance is:

$$[SO_4^{2-}]_{HIriv} = [SO_4^{2-}]_{atm} + [SO_4^{2-}]_{LTwea} + [SO_4^{2-}]_{spring} + [SO_4^{2-}]_{HI-rock} \quad (11)$$

With $[SO_4^{2-}]_{atm}$ calculated using equation (5) and $[SO_4^{2-}]_{spring}$ calculated using equation (10).

We consider that the $[SO_4^{2-}]_{LTwea}$ in HI rivers is relatively close to the $[SO_4^{2-}]_{LTwea}$ estimated in adjacent NI rivers. In S-rich magma contexts like subduction-related volcanoes, the low $[SO_4^{2-}]_{LTwea}$ contents result from the weathering of silicate minerals containing traces of S-rich inclusions (e.g. Parat et al., 2002; Metcalfe et al., 2022). The concentration of dissolved elements in HI rivers resulting from low-temperature chemical weathering is equal to:

$$[X]_{LTwea} = [SO_4^{2-}]_{LTwea} \times (X/\ SO_4^{2-})_{LTwea\ (NIriv)} \quad (12)$$

We used the $[SO_4^{2-}]_{LTwea}$ value of the Moustique River to determine $[X]_{LTwea}$ for the Grande Plaine River, and values of Capesterre River for Rivière Rouge, Rivière Noire and Rivière Galion (respectively 19.9 and 5.4 µmol/L). This choice allows us to compare watersheds flowing through the same lithology and soil.

For all rivers, the total dissolved solid values (mg/L) are equal to:

$$TDS = \Sigma[X] \quad (13)$$

The chemical rates expressed in t/yr were determined from TDS concentrations, runoff and watershed area. The rates expressed in t/km^2/yr were determined from TDS concentrations and runoff (Table 4).

4. Results

4.1. Hydrothermal spring waters

The temperatures of the four hydrothermal springs range from 29.2 to 46.9°C, and their pH values range from 4.9 and 6.6 (Table 2). The springs (sampled in 2013 and 2014) exhibit values within the range of previously reported values (Villemant et al., 2014).

The springs are characterized by high ionic concentrations (Table 2 and Fig. 2). Cl^- and SO_4^{2-} are the dominant anions (232–9976 and 210–7074 µmol/L, respectively), followed by HCO_3^- (140–1834 µmol/L). Na^+ and Ca^{2+} are the dominant cations (1112–2592 and 520–7064 µmol/L, respectively), followed by Mg^{2+} (212–2767 µmol/L) and K^+ (89–474 µmol/L). The Habitation Revel (HR) thermal spring is the least mineralized and presents a relatively stable chemical composition through time (e.g. Bigot et al., 1994; Villemant et al., 2014). Its Ca-Na-HCO_3 composition suggests a shallow origin of the water, which is heated via conductive heat transfer from La Soufrière volcano. In agreement with previous studies, the Galion (GA) and Ravine-Marchand (RM3) springs have a Ca-SO_4-Cl composition whereas the Bains-Jaunes (BJB) spring has a Ca-Na-SO_4-Cl composition. These water compositions result from absorption of volcanic vapors or water–rock interactions with shallow groundwaters. Since the mild reactivation of fumarolic activity in 1990, periodic analysis of the springs has shown a remarkable chemical evolution, mostly marked by an evolution in Cl content (Villemant et al., 2014; Li et al., 2015). This evolution has mainly been observed in GA, with a culminating Cl content in 2009, and a gradual decrease until 2014, the time of our study. This Cl anomaly has been observed to a lesser extent in BJB, with a very slight increase of Cl content observed until 2011, followed by a gradual decrease. Concerning the RM3 spring, a gradual slight increase in Cl content was still in progress in 2014 at the time of the sampling.

Lithium concentrations ranged from 1.2 to 2.5 µmol/L. The δ^7Li values varied between 8.3‰ and 13‰ and were slightly higher than isotopic ratios previously reported in other springs in Guadeloupe and Martinique (from 1 to 6‰; Millot et al., 2010a; Rad et al., 2013). Our values are also in the high range of Li isotopic data for hydrothermal springs reported in the literature for worldwide geothermal waters (e.g. Henchiri et al., 2014; Pogge von Strandmann et al., 2016; Bénard et al., 2020).

4.2. River waters

Two types of rivers can be distinguished: (1) rivers without hydrothermal influence (called non-impacted NI rivers); and (2) rivers that are partially affected by hydrothermal inputs (called hydrothermal-impacted HI rivers). The HI rivers are located around the fossil system of Les Mamelles (Grande-Plaine River), the fossil system of Carmichael (Rivière Rouge) and the active system of La Soufrière Volcano (Rivière Galion and Rivière Noire). The chemical composition of HI rivers is attributed to the leaching and dissolution of clay-rich, hydrothermally-

Table 4

Site	Li riv* kg/yr	Li riv* kg/km^2/yr	TDS riv* t/yr	TDS LT-wea* t/yr	TDS HI-rock* t/yr	TDS spring* t/yr	Cat WR* t/km^2/yr	CWR* t/km^2/yr	CWR** t/km^2/yr
Northern rivers									
Nogent	3.07	0.59	380	184	–	–	3.0	35.5	
Moustique Sainte-Rose	4.88	0.79	624	242	–	–	5.2	39.0	
Deshaies	1.39	0.32	229	113	–	–	2.9	25.7	
Central rivers									
Grande-Plaine	20.54	1.90	2390	389	1121	–			
Bras-David	3.99	0.36	1140	461	–	–	9.8	41.9	51.7
Quiock Creek	0.03	0.36	2.38	0.78	–	–	0.4	9.8	
Southern rivers									
Vieux-Habitants	11.29	0.59	4008	1963	–	–	25.3	102.8	84.6
Capesterre	6.62	0.41	3301	1449	–	–	21.4	89.4	91.8
Rivière Rouge	6.40	2.66	952	202	647	–			
Rivière Noire	7.40	6.16	654	101	85	266			
Galion	16.41	5.47	925	252	105	269			

*: Mean rates determined from data of this study.
**: Mean annual rates determined by Dessert et al. (2015) from total riverine concentrations and total water discharges, between 2007 and 2012.

altered rocks (fossil hydrothermal system) and/or to the discharge of thermal springs (active hydrothermal system).

In Fig. 2, HI rivers were distinguished from NI rivers. In NI river samples, pH varied between 4.6 in Quiock Creek and 7.8 in the Vieux-Habitants River. In HI river samples, pH was slightly more acidic and varied between 3.7 in Rivière Rouge and 7.4 in Rivière Noire. The chemical composition of HI rivers was clearly distinct from NI rivers (Table 2 and Fig. 2). The HI rivers were globally more concentrated in major and trace elements compared to NI rivers. They were characterized by SO_4^{2-} and Ca^{2+} concentrations higher than 100 μmol/L, resulting from the weathering of high-temperature hydrothermal minerals (as clay, pyrite, gypsum). Note the particularly high Cl^- content in Rivière Galion (266 to 1083 μmol/L), influenced by the Galion Spring enriched in dissolved volcanic gas (Villemant et al., 2014). Apart from the rivers directly influenced by the active system of La Soufrière, all the other rivers were characterized by oceanic Cl, with concentrations lower than 500 μmol/L on the northern island and lower than 150 μmol/L on the central-southern island. This north–south variation in Cl^- concentration has been previously interpreted as the effect of the evapotranspiration factor (from 4 in the north to 1.2 in the south; Lloret et al., 2011; Dessert et al., 2015). In NI rivers, Na^+ was the most abundant cation, ranging from 113 μmol/L in the Capesterre River during a flood event to 600 μmol/L in the Deshaies River. SiO_2 was also an abundant element in waters and varied between 102 μmol/L in the Bras-David River (during a flood event) or 109 μmol/L in Quiock Creek and 855 μmol/L in the Deshaies River. All our observations are in good agreement with those previously reported in studies on Guadeloupean rivers (Rad et al., 2006; Gaillardet et al., 2011; Lloret et al., 2011; Rivé et al., 2013; Dessert et al., 2015; Gaspard et al., 2021).

We observed a relatively large variability in Li concentrations and δ^7Li values in rivers in Guadeloupe (Fig. 2). HI rivers were the most concentrated and were characterized by the lightest δ^7Li isotopic ratio (from 3.1 to 12.3‰). Inversely, NI rivers were more diluted and isotopically heavier (16.0 to 31.6‰), except for Quiock Creek (7.2 to 9.3‰). This is consistent with values measured in tropical rivers draining andesitic or basaltic islands (e.g. Martinique, Réunion and Puerto Rico; Rad et al., 2013; Henchiri et al., 2014; Chapela Lara et al., 2022).

5. Discussion

5.1. High-temperature water–rock interactions

The Fig. 3 presents the Li isotopic composition for various waters from Guadeloupe plotted against the Li/Na (nmol/μmol) and the Cl/Li (μmol/nmol) ratios. The hydrothermal springs displayed high Li/Na, emphasizing that Li from seawater does not contribute significantly to these fluids (Li/Na = 0.08 and Cl/Li = 15.8 for seawater in Guadeloupe; Millot et al., 2010a) and that they are mainly influenced by high-temperature water–rock interactions.

The comparison between hydrothermal springs and their corresponding andesitic parent rock (Fig. 3) shows that δ^7Li values for spring water around the La Soufrière volcano are slightly heavier than those of the parent rock (5.3‰; Clergue et al., 2015). Such a result confirms that the preferential release of the heavy isotope (^{7}Li) is into the water. However, at high temperatures the isotopic fractionation is limited, with $\Delta^7Li_{water\text{-}andesite}$ ($\Delta^7Li_{water\text{-}andesite} = \delta^7Li_{water} - \delta^7Li_{andesite}$) values ranging between +3‰ and +7.7‰ in our samples, which is in good agreement with previous studies showing limited fractionation during high-temperature water–rock interactions (e.g. Bénard et al., 2020; Henchiri et al., 2014; Millot et al., 2010, 2012, Pogge von Strandmann et al., 2006, 2016; Zhang et al., 2022b). To constrain the controls on Li isotope fractionation in hot springs, we draw on insights from prior experimental and field studies, as discussed below. The fractionation of Li isotopes during water–rock interaction can vary as a function of the type of hydrothermal clays that release or incorporate lithium which itself depends upon the reaction temperature (Franzson et al., 2008; Verney-Carron et al., 2015). Experimental and field-based studies (e.g. Williams and Hervig, 2005; Vigier et al., 2008; Millot et al., 2010a; Verney-Carron et al., 2011, 2015) have shown that the Li isotopic fractionation factor inversely correlates with temperature during the formation of Li-bearing secondary minerals (e.g. $\Delta^7Li_{smectite\text{-}solution}$ of −1.6‰ at 250°C as opposed to −10‰ at 90°C, Vigier et a., 2008). There are few Li isotopic data for natural solids altered at high temperatures (e.g. Chan et al., 1994; Verney-Carron et al., 2015; Bobos and Williams, 2017), but with some evidence for Li enrichment in secondary phases, especially at temperatures higher than 250°C (Verney-Carron et al., 2015).

Because Li presents a low reactivity during fluid ascent up to the surface, it can be used as geothermometer, in particular using empirical Na/Li and Li isotope geothermometric relationships for hydrothermal fluids (e.g. Fouillac and Michard, 1981; Kharaka et al., 1982; Sanjuan et al., 2014; Millot et al. 2010a). In the hydrothermal waters of La Soufrière, Ruzié et al. (2013) determined the proportion of magmatic signal from the He isotopic ratio measured in waters. This magmatic component is dominant in RM3 (100 % of dissolved He) and GA (90–95 %) spring waters, showing that a deep aquifer has been sampled, with minimal dilution by meteoric water. This study also showed that, for BJ and HR springs, the dilution of the magmatic signal is significant, suggesting a contribution from a meteoric or organic component. We then only applied the Na/Li geothermometer ($T(K) = 2002/[\log(Na/Li)_{spring}$

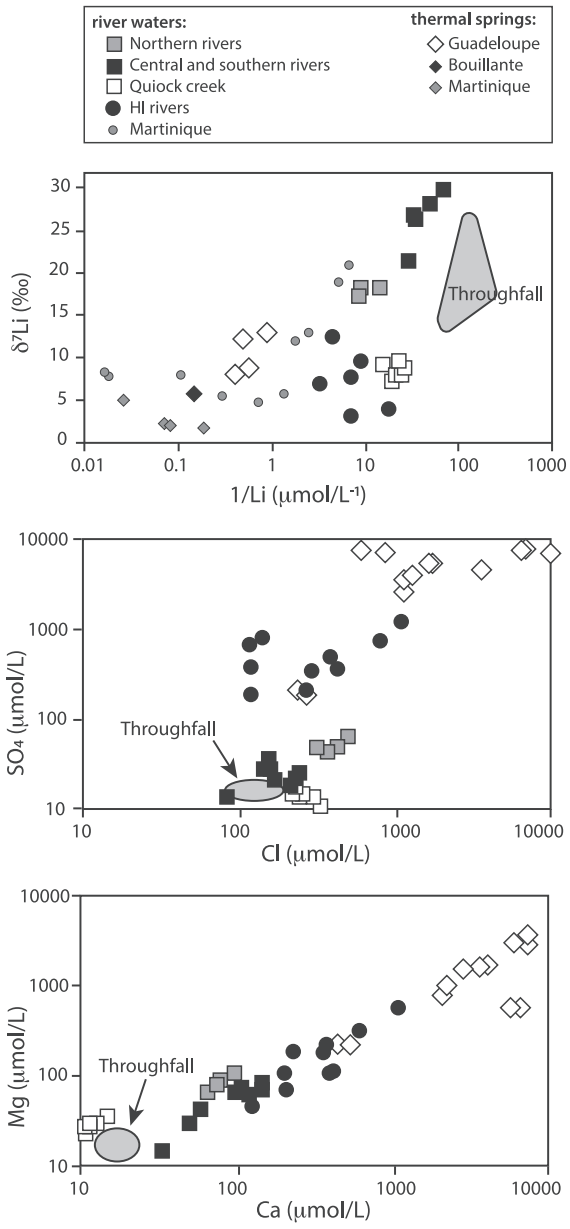

Fig. 2. (a) Lithium isotopic ratios (δ^7Li) against the 1/Li molar ratio in waters from Guadeloupe. Data from the literature have been added for comparison: Bouillante spring (Millot et al., 2010a), Ravine Quiock (river and throughfall; Clergue et al., 2015; Fries et al., 2019) and waters from Martinique (Rad et al., 2013). (b) SO_4 concentrations plotted as a function of Cl concentrations. (c) Mg concentrations plotted as a function of Ca concentrations (additional data are from Rivé et al., 2013; Dessert et al., 2015).

+ 1.322]; Sanjuan et al., 2014) and the δ^7Li geothermometer (T(K) = 7847/[δ^7Li $_{spring}$ − δ^7Li$_{rock}$ + 8.093]; Millot et al., 2010a) on GA et RM3 springs. The estimated temperature of the reservoir source is different depending on the geothermometer used: temperature varies between 156°C ($T_{Na/Li}$) and 224°C ($T_{\delta 7Li}$) for GA and between 190°C ($T_{Na/Li}$) and 253°C ($T_{\delta 7Li}$) for RM3. This temperature range is consistent with those previously estimated in gas samples from the summit fumerolic events (190-260°C; Brombach et al., 2000). More measurements of Li in the springs of La Soufrière volcano would confirm the robustness of these geothermometers and would add new constraints to the understanding of Li behavior in volcanic arc systems in tropical context.

5.2. Origin of dissolved Li in river water

In such a volcanic and tropical context, potential sources of dissolved Li include atmospheric deposits and water–rock interactions (both low-temperature and high-temperature).

Previous studies (Clergue et al., 2015; Dessert et al., 2015; 2020; Fries et al., 2019) have emphasized the significant effect of atmospheric inputs on the chemistry of rivers in Guadeloupe, particularly in the central and northern part of the island where a deep base cation-depleted regolith prevents roots to access to nutrients. Among the rivers not impacted by hydrothermal input, the Capesterre River had the highest Li isotopic composition, close to seawater (29.3‰; Millot et al., 2010a). The other NI rivers had δ^7Li values close to the throughfall signature, i.e. the atmospheric signature above the canopy (Fig. 3; Clergue et al., 2025). However, the Cl/Li ratios of these rivers are significantly lower than the Cl/Li ratios of atmospheric deposits, indicating a supplementary source of Li in the river waters. One exception is Quiock Creek, presenting a chemical and isotopic composition very close to the mixing curve between soil/regolith minerals and throughfall. An estimation of the atmospheric contribution can be obtained using the measured Cl concentrations and the atmospheric Li/Cl ratio (mean Li/Cl = 5.8 10^{-5}; Clergue et al., 2015), assuming that all of the Cl in the dissolved load has an atmospheric origin and a conservative behavior (equ. 5). Note that this calculation assumes that no atmospheric Li is incorporated into soil-forming secondary minerals, and hence is a maximum estimate of atmospheric Li contribution. The proportion of atmospheric Li in NI rivers varies between 23 % in the Nogent River and 34 % in Quiock Creek (Fig. 4 and Table 3). The highest atmospheric influence is in the Bras-David River, ranging between 44 % and 66 % during a flood event and resulting from strong rain events. The proportion of atmospheric Li is significantly lower in HI rivers, varying from 3 % in Rivière Noire to 16 % in Grande-Plaine River but still significant compared to other settings like the Amazon basin (0.1 to 2 %; Dellinger et al., 2015). This atmospheric input represents between 11 % and 67 % of the TDS, in Rivière Rouge and Quiock Creek respectively (Fig. 4 and Table 3).

Another important source of dissolved Li in river water is the discharge of thermal springs on La Soufrière volcano. Two rivers flowing through the southern flank of the volcano are impacted by this input: the Rivière Galion and Rivière Noire. These HI rivers are enriched in Li and are characterized by a high Li/Na ratio close to that of thermal springs (Fig. 3). These two rivers also have a Cl^- content higher than that of the atmosphere, suggesting that part of the riverine Cl^- content is derived from high-temperature fluids enriched with dissolved volcanic gas. This input from springs represents between 22 % and 44 % of the Li content and between 29 % and 41 % of the TDS, in Rivière Galion and Rivière Noire respectively (Fig. 4). In HI rivers, the riverine dissolved load is also influenced by the leaching and dissolution of clay-rich, hydrothermally-altered rocks ($C_{HI\text{-}rock}$). Because hydrothermal clays, that were formed during past hydrothermal activity, are strongly enriched in Li, their leaching and dissolution represent a significant Li input, characterized by a low δ^7Li isotopic ratio (e.g. Chan et al., 1994; Verney-Carron et al., 2015; Bobos and Williams, 2017). This process (HI-rock; Fig. 4 and Annexe Tab.1) explains between 46 % and 69 % of the dissolved Li content and between 11 % and 68 % of the TDS. Altogether, we show that the input of hydrothermal Li (spring + HI-rock) is a major part of the dissolved Li in HI rivers (between 55 and 89 %), confirming previous studies on rivers in a volcanic context (Pogge von Strandmann et al., 2006; Rad et al., 2013; Henchiri et al., 2014). This hydrothermal input also strongly influences the δ^7Li of the HI rivers. The study by Henchiri et al. (2014) on the rivers on the volcanic island of La Réunion showed an inverse correlation between riverine δ^7Li and the proportion of Li coming from hydrothermal inputs. This relationship is also observed in the rivers in Guadeloupe, where the lowest δ^7Li ratio has been measured in rivers impacted by hydrothermal input (3.5 to 12.4‰). The δ^7Li of the riverine dissolved phase (coupled with the Na/Li ratio) is therefore a

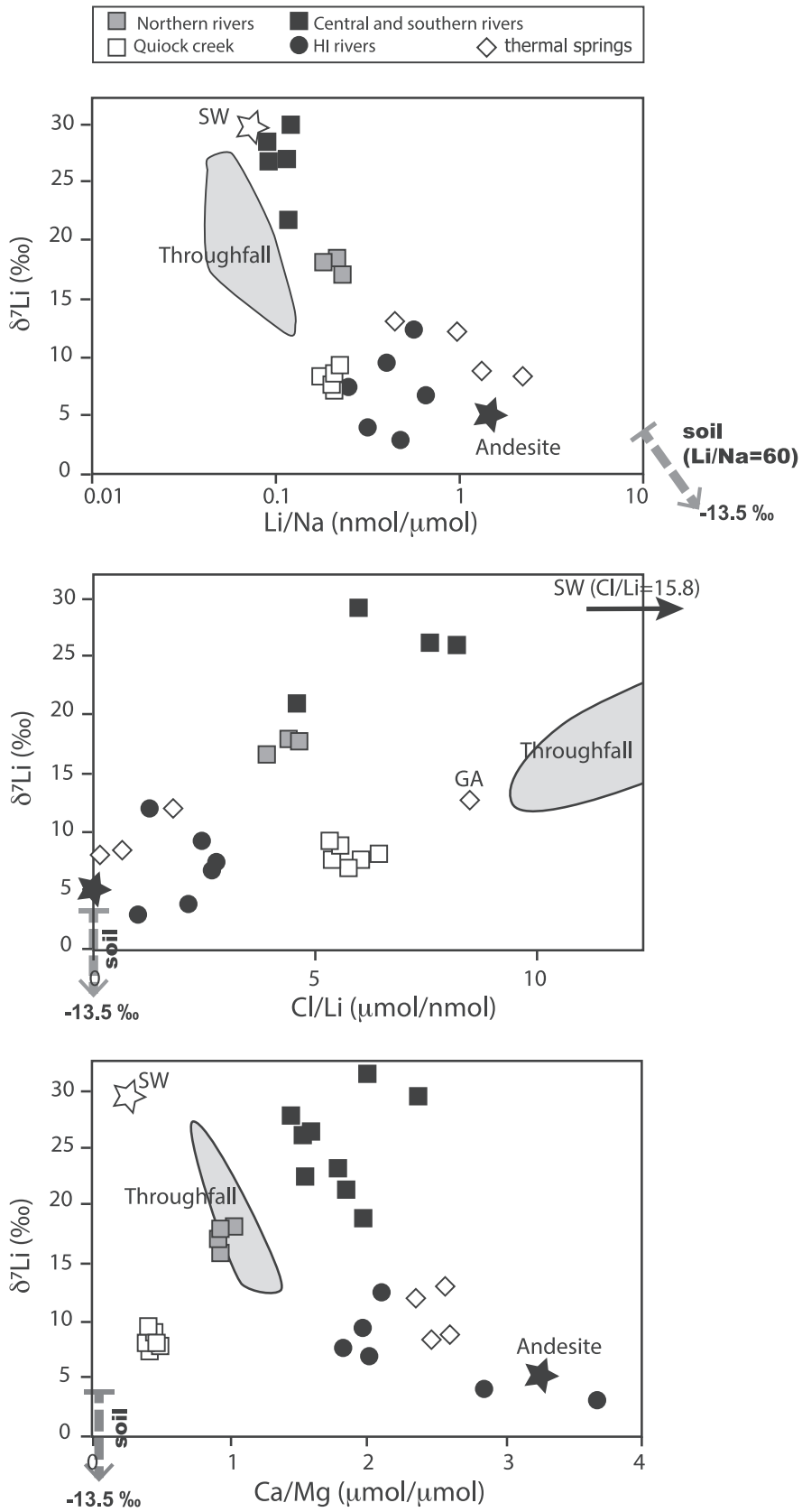

Fig. 3. Lithium isotopic ratios as a function of Na/Li, Cl/Li or Ca/Mg molar ratios in all river samples (HI and NI rivers, respectively illustrated by circles and squares) and in hot springs (GA, RM3, BJ and HR; illustrated by diamonds). Data for andesite and ferralitic regolith are from Clergue et al., 2015.

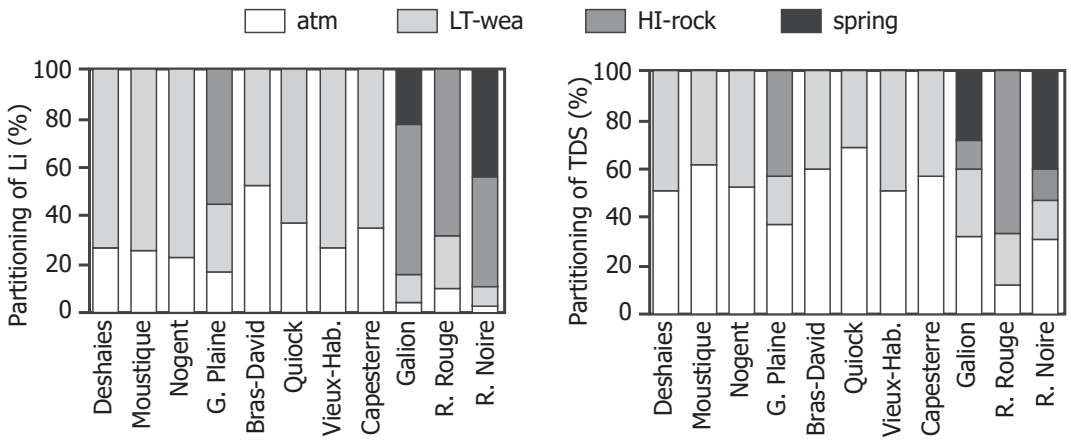

Fig. 4. Partitioning of Li and TDS deriving from each source.

good tracer of hydrothermal input, which could be very useful for geothermal prospection.

Finally, our calculations show that the low-temperature chemical weathering process (LT-wea) is a major source of Li in NI rivers (47 to 77 %) that decreases significantly in HI rivers (8 to 28 %). The low-temperature weathering process explains between 33 and 50 % of the TDS of NI rivers and only 16 to 27 % of the TDS of HI rivers.

Overall, our results show that the sources of dissolved Li vary significantly across the small tropical volcanic island of Basse-Terre. In contrast to most other settings, the Li atmospheric contribution to the river dissolved load is large (3 to 50 %) and cannot be neglected. The riverine δ^7Li is very sensitive to hydrothermal input and seems to be a good geothermal prospecting tool. Because the flux of the hydrothermal resurgences is integrated into the global riverine flux, the chemical budget can be used to estimate the first order weathering rate of the volcano (Table 3).

5.3. *Controls on Li fractionation processes during low-temperature weathering*

In this section, we focus on NI rivers (no hydrothermal inputs). Values of δ^7Li in NI rivers are highly variable at the scale of Basse-Terre Island, ranging from 8.2‰ in Quiock Creek to 31.6‰ in the Capesterre River, and are significantly higher than those of the andesitic source rock (5.3‰; Clergue et al., 2015). This result confirms that a large fractionation of Li isotopes occurs during weathering processes and specifically during the incorporation of Li in secondary minerals.

To understand the impact of secondary minerals on δ^7Li of the NI riverine dissolved load, we used the (Li/Na) ratio (Millot et al. 2010b). Indeed, Li and Na have the same behavior during andesite dissolution and are released into solution at the same rate (Verney-Carron et al., 2011). However, because of the strong affinity of Li for clays and oxy-hydroxides, Li is re-incorporated into secondary minerals, contrary to Na which remains in solution (e.g. Sawhney, 1972). We calculate the fraction of Li left in solution after secondary mineral precipitation (f_{Li}) by comparing the Li/Na ratio in the residual solution to the Li/Na in the initial solution (Millot et al., 2010b; Henchiri et al., 2014; Dellinger et al., 2015):

$$f_{Li} = (Li/Na)_{residual} / (Li/Na)_{initial} \quad (14)$$

A f_{Li} value of 0 means that all the Li present in the initial solution is re-incorporated into secondary minerals while a f_{Li} value of 1 means that Li is not re-incorporated into secondary minerals after its initial dissolution. We used both steady-state open system ("batch" model) and Rayleigh distillation models to explain the δ^7Li of the dissolved load of rivers compared to the source rock (e.g. Huh et al., 2001; Kisakurek et al., 2005; Vigier et al., 2009; Dellinger et al., 2015; Pogge von Strandmann et al., 2019). For the Rayleigh model, the evolution of the Li isotopic composition of the residual solution as a function of f_{Li} is given by the following equation:

$$\delta^7Li_{residual} = \delta^7Li_{initial} + 1000(\alpha_{clay-water} - 1) \times \ln(f_{Li}) \quad (15)$$

The fractionation factor $\alpha_{clay\text{-}water}$ is the isotopic shift occurring during the incorporation of Li into secondary minerals ($\Delta_{clay\text{-}water} = 1000 \ln\alpha$).

For the steady-state open system model, the evolution of the Li isotopic composition of the residual solution as a function of f_{Li} is given by the following equation:

$$\delta^7Li_{residual} = \delta^7Li_{initial} + 1000(\alpha_{clay-water} - 1) \times (1 - f_{Li}) \quad (16)$$

In Guadeloupe, a significant proportion of dissolved Li is derived from atmospheric input (see section 2 in the discussion above). To determine the proportion of Li^+ incorporated into secondary minerals, we consider that all the wet atmospheric inputs (rainwater) percolate through the weathering zone before entering the rivers (Guérin et al., 2019). In that scenario, secondary weathering minerals form from a solution that corresponds to a mixture of dissolved ions derived from both mineral dissolution and from atmospheric inputs. The mass-balance for the concentration of initially dissolved lithium (before incorporation into secondary minerals) in NI rivers is:

$$[Li]^0_{riv} = [Li]^0_{atm} + [Li]^0_{LTwea} \quad (17)$$

The initial Li concentration derived from atmospheric ($[Li]^0_{atm}$) and low-temperature andesite dissolution ($[Li]^0_{LTwea}$) can be calculated using the following equations:

$$[Li]^0_{atm} = [Na]_{atm} \times \left(\frac{Li}{Na}\right)_{Rain} \quad (18)$$

$$[Li]^0_{LTwea} = [Na]_{LTwea} \times \left(\frac{Li}{Na}\right)_{Andesite} \quad (19)$$

With $(Li/Na)_{Andesite} = 1.46 \times 10^{-3}$ mol.mol^{-1} and $(Li/Na)_{Rain} = 7.02 \pm 0.15 \times 10^{-5}$ mol.mol^{-1} (Clergue et al., 2015). This value for rainwater is derived from rain and throughfall samples (n = 48) collected in Quiock Creek and corresponds to 75±15 % proportion of Li derived from sea salt and 25±15 % derived from leaching of saharan dusts (Clergue et al., 2015).

We can use the mixing proportion for sodium (γ^{Na}_{atm} and γ^{Na}_{LTwea}; equations 7 and 8) to quantify the initial $(Li/Na)_0$ for each NI river:

$$\left(\frac{Li}{Na}\right)_0 = \left(\frac{Li}{Na}\right)_{Andesite} \gamma^{Na}_{LTwea} + \left(\frac{Li}{Na}\right)_{Rain} \gamma^{Na}_{atm} \quad (20)$$

The Li isotopic composition (δ^7Li_0) of the initial solution (before secondary mineral precipitation) is:

$$\delta^7 Li_0 = \delta^7 Li_{Andesite} \times \gamma^{Li0}_{LTwea} + \delta^7 Li_{Rain} \times \gamma^{Li0}_{atm} \quad (21)$$

With $\delta^7Li_{Andesite} = +5.3‰$ and $\delta^7Li_{Rain} = +23.1 \pm 4.8‰$ (Clergue et al., 2015).

The isotopic composition of the residual solution for the Rayleigh model is assumed to be equivalent to those of river water, so equation (15) becomes:

$$\delta^7Li_{river} = \delta^7Li_0 + 1000(\alpha_{clay-water} - 1) \times \ln(f_{Li}) \quad (22)$$

The isotopic composition of the residual solution for the "batch" model is assumed to be equivalent to those of river water, so equation (16) becomes:

$$\delta^7Li_{river} = \delta^7Li_0 + 1000(\alpha_{clay-water} - 1) \times (1 - f_{Li}) \quad (23)$$

Fig. 5 presents the evolution of the δ^7Li_{river}- δ^7Li_0 (the Li fractionation during its incorporation into secondary minerals) as a function of f_{Li} predicted by both the Rayleigh and batch models at different fractionation factors $\alpha_{clay\text{-}water}$. The $\alpha_{clay\text{-}water}$ factor varies between 0.975 (Pistiner and Henderson, 2003) and 0.988 (Millot and Girard, 2007) for gibbsite and is equal to 0.993 for kaolinite (Millot and Girard, 2007; Li and Liu, 2020).

For the southern and central rivers, the f_{Li} factor is between 0.15 and 0.23 for Vieux-Habitants River (VH) and Capesterre River (CAP), meaning that 85 % and 77 % of the initial Li is incorporated into secondary minerals. The f_{Li} factor determined for Bras-David River (BD) is higher and varies between 0.20 and 0.45. This large variability for BD may be linked to the hydrologic stage of the river, lowest δ^7Li_{river} and highest f_{Li} (0.45) corresponding to a flood water sample. A decrease of δ^7Li_{river} during storms has already been observed in Elder Creek (California, USA) by Golla et al. (2022). The authors explained the isotopic shift during flood as the result of the increase of groundwater flow rates and/or a greater contribution of Li from the sub-surface regolith with limited incorporation of Li into secondary minerals. In Guadeloupe, Guérin et al. (2019) have shown that, during strong rain events, the percolation of water through the regolith is also more important, inducing a shorter transit time of fluid through the sub-surface regolith. The greater influence of shallow groundwaters during floods in Guadeloupe was also emphasized by Lloret et al. (2011), who have measured enrichment into dissolved soil organic carbon during storms.

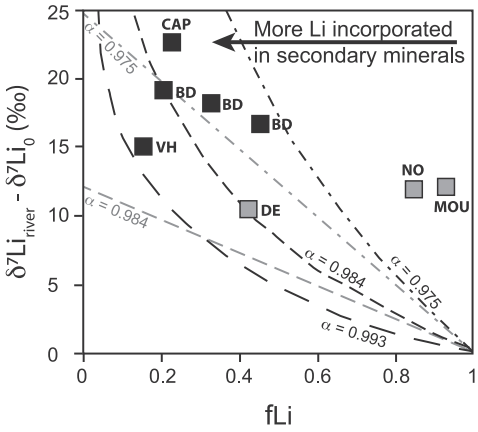

Fig. 5. Estimated lithium isotopic ratios (δ^7Li_{river}-δ^7Li_0) vs. the fraction of Li remaining in solution (f_{Li}) after secondary mineral precipitation. The curves represent the evolution of δ^7Li vs. f_{Li} predicted by the Rayleigh model (in black) and steady-state open system model (in grey) at different fractionation factors $\alpha_{clay\text{-}water}$. The fractionation factor α varies between 0.975 (Pistiner and Henderson, 2003) and 0.988 (Millot and Girard, 2007) for gibbsite and is close to 0.993 for kaolinite (Millot and Girard, 2007). The models explain the signatures of the central and southern rivers with α consistent with values in the literature. Only the data from NI rivers are represented on this figure.

The southern and central rivers of Basse-Terre Island can be described by the Rayleigh model, with a fractionation factor $\alpha_{clay\text{-}water}$ varying between 0.979 and 0.992, consistent with the mineralogy of the soils and the regolith on the volcanic island.

The northern rivers, flowing through the oldest part of the island have very different characteristics. First, they have lower δ^7Li_{river}- δ^7Li_0 values and higher f_{Li} values relative to southern and central rivers. This shows that the incorporation of Li into secondary minerals is reduced in this context. Second, we note that the isotopic composition of the Moustique River (MOU) and Nogent River (NO) cannot be explained by the Rayleigh model and that another process is required. In the highly weathered ferralitic catchment of Quiock Creek, we have previously showed that the secondary mineral dissolution was a major solute source for this small watershed (8 ha) and that andesite no longer participated in significant production of cations and Li (Clergue et al., 2015; Fries et al., 2019; Dessert et al., 2020). The Quiock Creek is characterized by a $f_{Li} > 1$ and a very low δ^7Li ratio (8.2‰) associated with a transport-limited weathering regime. Due to the presence of a deep and highly weathered regolith in the northern catchments, the dissolution of previously-formed secondary minerals could partially explain why the Nogent and Moustique Rivers have f_{Li} close to 1 and do not plot on the same trend on Fig. 5, i.e., the $(Li/Na)_0$ is higher than $(Li/Na)_{andesite}$ due to the contribution of older clays with high Li/Na. Such influence of regolith-derived secondary minerals on the riverine budget in Guadeloupe has also been shown with Mg isotopes in previous studies (Dessert et al., 2015; Fries et al., 2019).

The effect of secondary mineral dissolution on dissolved δ^7Li values was also studied in the highly weathered catchment of Bisley in Puerto Rico (Chapela Lara et al., 2022). Quiock Creek and Bisley catchments are relatively similar, with small surface (respectively 8 and 7 ha), underlain by andesitic bedrock and covered by deep (>10 m) highly weathered regolith under a wet tropical climate. From the Li isotopic composition of both the solid and liquid products of the weathering regolith profile, the authors have shown that dissolution of secondary minerals produced porewaters enriched in ^{6}Li. However, the extremely low δ^7Li values of porewater (−27 to + 8‰) are not reflected in the δ^7Li signature of the local Bisley stream (+32 to + 37‰), indicating that stream water is not directly impacted by the regolith porewaters. The reason for this apparent decoupling between the Li signature of porewater and Bisley stream water was not definitively established by the authors, who mentioned the hydrological setting. In contrast to what we observe in Quiock Creek river, the Bisley stream is not influenced by shallow porewaters but is influenced by deeper groundwaters, reflecting reactions along water pathways in the deep regolith, where relatively Li-rich primary minerals are still being altered.

In summary, our results have shown that secondary minerals played a critical role in the Li isotopic signature of the rivers of Basse-Terre Island. We interpret this large δ^7Li offset as resulting from two distinct weathering processes in the regolith. In the central and southern parts of the island, the rivers were characterized by high δ^7Li values, emphasizing that dissolved Li is mainly driven by the very efficient incorporation of Li into secondary minerals (around 80 % of the dissolved Li) that preferentially incorporated ^{6}Li. In the northern part of the island, the rivers were characterized by lower δ^7Li values, which were partly attributed to a low δ^7Li source coming from the dissolution of secondary minerals contained in the regolith (the δ^7Li values of ferralitic regolith in Guadeloupe ranged between + 3.9 and −13.5‰; Clergue et al., 2015). Overall, the balance between Li dissolution and its incorporation into secondary minerals varies from north to south, following the bedrock age gradient, and accounts for the diversity of δ^7Li signatures of the NI rivers in Guadeloupe.

5.4. Relation between the δ^7Li ratio and the low-temperature weathering rate

The chemical weathering rate (CWR) of NI rivers ranges between 9.8 t/km^2/yr for Quiock Creek and 102.8 t/km^2/yr for the Vieux-Habitants River (Table 3; Fig. 6). The North–South weathering gradient on Basse-Terre Island has already been documented in previous studies (e.g. Gaillardet et al., 2011; Lloret et al., 2011; Dessert et al., 2015). Except for Quiock Creek, the lowest rates were measured in the northern, oldest part of the island (rock age > 2 Ma; Table 1), where thick ferralitic regoliths are mainly constituted of secondary minerals such as clays and iron oxides (Fig. 7). The northern watersheds are also characterized by moderate topography (only 3 to 7 % of the watershed surface are slopes > 49 %) and moderate precipitation (<3000 mm/yr) and runoff, which contributes to reduced weathering processes. The chemical weathering rates are greater in the central part of the island (Bras-David River) and the highest values are in the youngest, Southern area, where the pool of weatherable primary minerals (contained in ferralitic regoliths and Andosols) is the highest (Henriet et al., 2008). These central and southern watersheds are also characterized by high topography (14 to 55 % of the watershed surface are slopes > 49 %) and high precipitation (>3500 mm/yr) and runoff, which all boost weathering processes.

A positive trend is observed between the δ^7Li ratios of rivers and the CWR for NI rivers (Fig. 6). The chemical and isotopic composition of the Northern rivers is significantly influenced by the dissolution of the secondary minerals contained in the old and highly depleted regoliths. Conversely, the rivers of the central and southern part of the island are mainly controlled by the dissolution of primary andesitic minerals and the formation of secondary minerals.

5.5. Comparison with other volcanic islands and global implications

In this section, we compare the results from Guadeloupe with other volcanic islands (Iceland and Hawaii). The Li-specific yield (kg/km^2/yr) of rivers in Basse-Terre, Guadeloupe, decreases with bedrock age (Table 4). Rivers draining the young Soufrière Volcano show Li yields (2–7 kg/km^2/yr) an order of magnitude higher than those draining older formations (>0.45 Myr; Li yield < 0.8 kg/km^2/yr). The main exception is the Grande Plaine River, whose elevated Li yield (1.9 kg/km^2/yr) reflects the dissolution of Li-rich hydrothermal clays from the fossil Les Mamelles hydrothermal system. This decline in Li-specific yield with bedrock age is consistent with observations from Icelandic rivers (Vigier et al., 2009; Pogge von Strandmann et al., 2023), and Hawaiian regolith (Ryu et al., 2014), where most Li depletion occurs within the first ~ 0.02

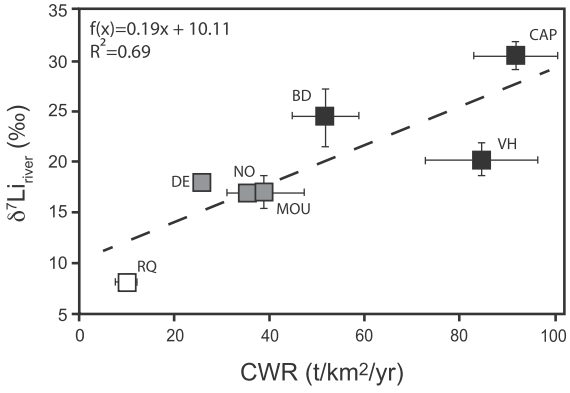

Fig. 6. Lithium isotopic ratios (δ^7Li) vs. chemical weathering rates (CWR in t/km^2/yr). CWR data from the Capesterre, Bras-David and Vieux-Habitants rivers are from Dessert et al. (2015). The topographic index is determined as the % of watersheds with slopes > 49 %. This index is equal to: 0 % for Quiock-Creek; 3 to 7 % for northern rivers; 14 % for Brad-David; 50 to 55 % for southern rivers (see Lloret et al., 2011 for details).

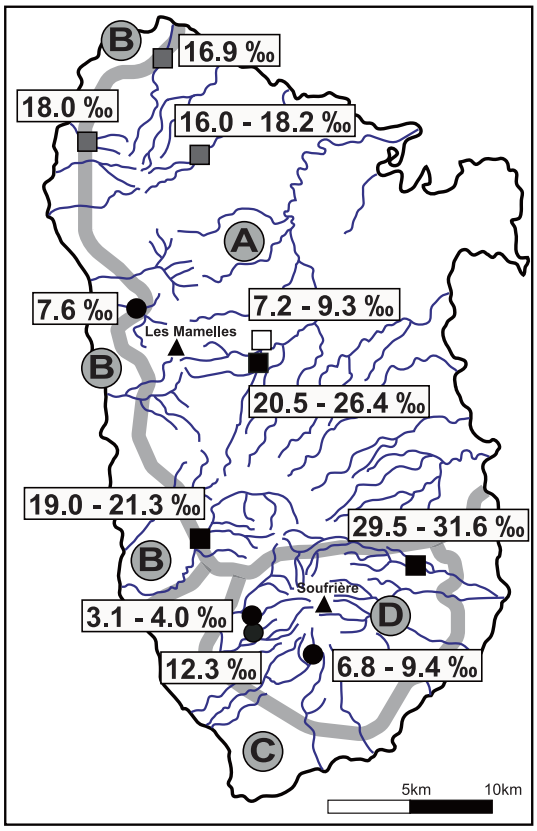

Fig. 7. Map of the dissolved lithium isotopic composition of rivers and the distribution of soil types (Colmet-Daage and Bernard, 1979). Soil types are related to rock age, precipitation and topography: (A) Ferralitic soils with iron oxides and kaolinite-halloysite; (B) Vertisols with Ca,Mg,Na smectites or Nitrisols with smectite and halloysite; (C) Andosols with allophanes; (D) young Nitrisols with halloysite. The substratum ages range from 4.3 to 1.1 Ma above the dotted line and are ≤ 0.9 Ma below this line (see Fig. 1). NI-rivers are represented by squares and HI-rivers by circles.

Myr. In Guadeloupe, high Li yields partly reflect inputs from active and extinct hydrothermal systems, whereas in Iceland they are mainly driven by the high reactivity of glassy basalts and possibly enhanced by intense physical erosion (Pogge von Strandmann et al., 2023; Louvat et al., 2008).

The temporal evolution of dissolved river δ^7Li with bedrock age in Guadeloupe shows a non-linear pattern similar to Hawaii (Ryu et al., 2014), with low δ^7Li during early (<0.45 Myr) and late (>2 Myr) stages of weathering. Early-stage weathering is dominated by rapid (high Li-specific yield), congruent dissolution with limited incorporation of Li in secondary minerals; in Guadeloupe, this is further promoted by high-temperature weathering (Henchiri et al., 2014). Maximum δ^7Li values, reflecting high Li sequestration into clays, occur at intermediate ages (between 0.45 and 1.15 Myr in Guadeloupe and ~ 1.4 Myr in Hawaii). The subsequent decline after ~2 Myr is consistent with clay re-dissolution (Ryu et al., 2014) and slow associated Li release (low Li-specific yield). As for the Li-specific yield, the Grande Plaine River also deviates from this trend with lower δ^7Li compared to other rivers of similar bedrock age.

Our study highlights a completely different story than that presented by Vigier et al. (2009) and Pogge von Strandmann et al. (2023) on the behavior of Li isotopes during weathering in Iceland's watersheds. In Iceland, high δ^7Li values are measured in rivers draining old (> 2 Myr) and weathered basalt catchments, whereas low δ^7Li values are (as in Guadeloupe) measured in rivers draining the younger parts of the island where the highest CWR values are recorded. In addition the dissolved δ^7Li of NI Rivers in Guadeloupe is positively correlated to average runoff

($r^2 = 0.58$, n = 7 rivers, not shown), which is the opposite of rivers from Iceland (Pogge von Strandmann et al., 2023) and at global scale (Zhang et al., 2022a). We justify these major differences in light of the weathering intensity described by Bouchez et al. (2014) and Dellinger et al. (2015). Unlike Guadeloupe, the regoliths in Iceland are thin and not highly depleted in Li (Pogge von Strandmann et al., 2021), with an important pool of weatherable primary minerals. The weathering regime in Iceland is of low to intermediate weathering intensity (Pogge von Strandmann et al., 2023), and the dissolved δ^7Li is mainly driven by two processes: Li release from primary minerals and Li uptake by secondary minerals. In Guadeloupe, the weathering intensity is intermediate in the south and high in the north of the island. In addition to primary mineral weathering and secondary mineral formation, a third key process – absent or minor in Iceland – controls the dissolved δ^7Li: the release of Li from Li-bearing soil secondary phases that have accumulated Li over long timescales. As a consequence, the dissolved δ^7Li in Guadeloupe is primarily controlled by the solid residence time and the long-term weathering intensity, rather than by modern hydrological parameters such as the fluid residence time. Because of the drastic difference in temperature and weathering regime, it is therefore not surprising to observe an inverse trend between Iceland and Guadeloupe.

Vigier et al. (2009) stated that their empirical law on the relationship between chemical weathering rate and dissolved δ^7Li may be applicable to most large scale watersheds. However, our results have shown that under a tropical regime with intermediate to high weathering intensity, the δ^7Li ratio behaves differently from that observed in Iceland. Early stage weathering on tropical volcanic islands produces both high Li yields and low δ^7Li values, similar to rivers draining high-elevation mountain belts (Zhang et al., 2022a). Our results therefore indicate that tropical volcanic settings can exert a large influence on the global Li flux and the δ^7Li composition of seawater (Henchiri et al., 2014), but only during the initial phase of weathering. Beyond this early stage, Li yield declines sharply and becomes comparable to those of rivers draining high weathering intensity (W/D) environments (Pogge von Strandmann et al., 2021). More studies on volcanic tropical islands are needed to improve our understanding of the global Li geochemical cycle and for better constraining past changes in continental weathering based on the record of past Li isotope compositions (Misra and Froelich, 2012; Pogge von Strandmann et al., 2013).

6. Conclusion

To better constrain the origin of dissolved Li and the behavior of Li isotopes during water–rock interactions in a tropical volcanic context, we sampled and measured river and hydrothermal spring waters on the volcanic island of Guadeloupe. The δ^7Li values measured in four hydrothermal springs around La Soufrière volcano are low and (between 8.3‰ and 13‰) in accordance with previous studies on other settings. We also observed a remarkable variability of the Li concentrations and δ^7Li values in rivers. The rivers affected by hydrothermal inputs have the highest Li concentration and lowest δ^7Li (from 3.1 to 12.3‰). Inversely, the rivers not impacted by hydrothermal inputs (NI rivers) were more diluted and isotopically heavier (7.2 to 9.3‰ for Quiock Creek; 16.0 to 31.6‰ for other rivers), highlighting different processes and degrees of weathering. We interpreted this large δ^7Li offset as resulting from two distinct weathering processes in the regolith, both driven by secondary minerals dynamics. In the central and southern parts of the island, the high δ^7Li values are explained by the dissolution of primary andesitic minerals and the very efficient incorporation of Li into secondary minerals (80 % of the initially dissolved Li) that preferentially incorporated ^{6}Li. In contrast, in the northern part of the island, the NI rivers are characterized by lower δ^7Li values which we attribute to a low δ^7Li source coming from the dissolution of secondary minerals contained in the regolith (the δ^7Li values of highly-weathered regoliths ranged between −13.5 and +3.9‰ Clergue et al., 2015). In Guadeloupe a positive relationship between δ^7Li of river waters and chemical weathering rates is observed and corresponds to the gradient of weatherable primary minerals in watersheds. We noted that this gradient is linked to rock age, precipitation, regolith thickness and geomorphologic parameters such as elevation and slope.

In a broader context, we have shown that, in Basse-Terre Island chemical weathering on a volcanic island could produce waters with a large range of Li contents and δ^7Li ratios, making the estimation of the Li riverine budget challenging. As volcanic and tropical zones contribute significantly to the global Li flux to the ocean (Henchiri et al., 2014), our study highlights the importance of further research to improve the understanding of the global riverine and oceanic Li budgets. That will be particularly useful for better constraining past changes in continental weathering based on the record of past Li isotope compositions.

Data availability

The data used in this manuscript is available through IPGP Research Collection (research-collection.ipgp.fr) at the following https://doi.org/10.18715/IPGP.2025.m91mz0xn.

CRediT authorship contribution statement

Céline Dessert: Writing – original draft, Validation, Supervision, Project administration, Funding acquisition, Data curation, Conceptualization. **Mathieu Dellinger:** Writing – review & editing, Validation, Methodology, Formal analysis. **Clémentine Clergue:** Writing – original draft, Validation, Methodology, Formal analysis. **Jérôme Gaillardet:** Writing – review & editing. **Marc F. Benedetti:** Writing – review & editing, Supervision, Funding acquisition.

Declaration of competing interest

The authors declare that they have no known competing financial interests or personal relationships that could have appeared to influence the work reported in this paper.

Acknowledgements

This work has been financially supported by the INSU-CNRS and the Region of Guadeloupe. Parts of this work were supported by the IPGP multidisciplinary program PARI and by the Paris–IdF region SESAME Grant no. 12015908. The study was also partly supported by IdEx Université de Paris ANR-18-IDEX-0001. This work could not have been done without logistical support from both INSU-CNRS observatories in Guadeloupe run by the IPGP: the Observatoire de l'Eau et de l'Erosion aux Antilles (OBSERA) and the Observatoire Volcanologique et Sismologique de Guadeloupe (OVSG). We thank the National Park of Guadeloupe which allows us to work in its protected area. This work was also supported by the European Research Council (ERC) under the European Union's Horizon Europe Research and Innovation Program (ERC Starting Grant LAKE-SWITCH, No. 101041998 to M.D.) and the ANR-DFG project (Grant ANR-22-CE92-0078, PALAVAS project). This study greatly benefited from comments from E. Lajeunesse, J. Bouchez, S. Henchiri and P. Louvat. A special acknowledgment is due to S. Johnson for her helpful comments on the original version of this paper. We gratefully acknowledge three anonymous reviewers and the editor for their helpful and critical comments on the original manuscript.

Appendix A. Supplementary material

The supplement contains the data Table A.1. including the mean source partitioning for each chemical species. Calculations are described in section 3.3. Supplementary material to this article can be found online at https://doi.org/10.1016/j.gca.2026.01.047.

References

Allemand, P., Delacourt, C., Lajeunesse, E., Devauchelle, O., Beauducel, F., 2014. Erosive effects of the storm Helena (1963) on Basse Terre Island (Guadeloupe — Lesser Antilles Arc). Geomorphology 206, 79–86.

Allemand, P., Lajeunesse, E., Devauchelle, O., Langlois, V., 2023. Entrainment and deposition of boulders in a gravel bed river. Earth Surf. Dyn. 11, 21–32.

Bénard, B., Famin, V., Agrinier, P., Aunay, B., Lebeau, G., Sanjuan, B., Dezayes, C., 2020. Origin and fate of hydrothermal fluids at Piton des Neiges volcano (Réunion Island): a geochemical and isotopic (O, H, C, Sr, Li, Cl) study of thermal springs. J. Volcanol. Geoth. Res. 392, 106682.

Berner, R.A., Lasaga, A.C., Garrels, R.M., 1983. The carbonate silicate geochemical cycle and its effect on atmospheric carbon dioxide over the past 100 million years. Am. J. Sci. 284, 641–683.

Bigot, S., Boudon, G., Semet, M. Hammouya G., 1994. Traçage chimique de la circulation des eaux souterraines sur le volcan de la Grande Découverte (La Soufrière), Guadeloupe. C. R. Acad. Sci. 318 (Series IIA), 1215–1221.

Bobos, I., Williams, L.B., 2017. Boron, lithium and nitrogen isotope geochemistry of NH4 illite clays in the fossil hydrothermal system of Harghita Băi, East Carpathians, Romania. Chem. Geol. 473, 22–39.

Bouchez, J., von Blanckenburg, F., Schuessler, J.A., 2013. Modeling novel stable isotope ratios in the weathering zone. Am. J. Sci. 313 (4), 267–308.

Bouchez, J., von Gaillardet, J., Blanckenburg, F., 2014. Weathering Intensity in Low land River Basins: from the Andes to the Amazon Mouth. Proc. Earth Planet. Sci. 10, 280–286.

Boudon, G., Komorowski, J.-C., Villemant, B.S., M.P., 2008. A new scenario for the last magmatic eruption of La Soufrière de Guadeloupe (Lesser Antilles) in 1530 A.D.: evidence from stratigraphy, radiocarbon dating and magmatic evolution of erupted products. J. Volcanol. Geoth. Res. 178, 474–490.

Brombach, T., Marini, L., Hunziker, J.C., 2000. Geochemistry of the thermal springs and fumaroles of Basse-Terre Island, Guadeloupe, Lesser Antilles. Bull. Volcanol. 61, 477–490.

Buss, H.L., Brantley, S.L., Scatena, F.N., Bazilievskaya, E.A., Blum, A., Schulz, M., et al., 2013. Probing the deep critical zone beneath the Luquillo experimental forest, Puerto Rico. Earth Surf. Proc. Land. 38 (10), 1170–1186.

Buss, H.L., White, A.F., Dessert, C., Gaillardet, J., Blum, A.E., Sak, P.B., 2010. Depth profiles in a tropical volcanic critical zone observatory: Basse-Terre, Guadeloupe. In: Torres-Alvarado, I.S., Birkkle, P., (Eds.), Proceedings of the 13th International Conference on Water-Rock Interaction. Taylor & FrancisGroup. London, UK.

Chan, L.H., Gieskes, J.M., You, C.F., Edmond, J.M., 1994. Lithium isotope geochemistry of sediments and hydrothermal fluids of the Guaymas Basin. Gulf of California. Geochim. Cosmochim. Acta 58, 4443–4454.

Chapela Lara, M., Buss, H.L., Henehan, M.J., Schuessler, J.A., McDowell, W.H., 2022. Secondary minerals drive extreme lithium isotope fractionation during tropical weathering. J. Geophys. Res. Earth 127, e2021JF006366.

Clergue, C., Dellinger, M., Buss, H.L., Gaillardet, J., Benedetti, M.F., Dessert, C., 2015. Influence of atmospheric deposits and secondary minerals on Li isotopes budget in a highly weathered catchment, Guadeloupe (Lesser Antilles). Chem. Geol. 414, 28–41.

Colmet-Daage, F., Bernard, Z., 1979. Contribution à l'Atlas des départements d'Outremer: Guadeloupe. Carte des sols de la Guadeloupe, Grande-Terre, Marie-Galante. Carte des pentes et du modelé de la Guadeloupe, Grande-Terre, Marie-Galante. ORSTOM, Antilles.

Coogan, L.A., Gillis, K.M., Pope, M., Spence, J., 2017. The role of low-temperature (off-axis) alteration of the oceanic crust in the global Li-cycle: Insights from the Troodos ophiolite. Geochim. Cosmochim. Acta 203, 201–215.

Dellinger, M., Gaillardet, J., Bouchez, J., Calmels, D., Galy, V., Hilton, R.G., Louvat, P., France- Lanord, C., 2014. Lithium isotopes in large rivers reveal the cannibalistic nature of modern continental weathering and erosion. Earth Planet. Sci. Lett. 401, 359–372.

Dellinger, M., Gaillardet, J., Bouchez, J., Calmels, D., Louvat, P., Dosseto, A., Gorge, C., Alanoca, L., Maurice, L., 2015. Riverine Li isotope fractionation in the Amazon River basin controlled by the weathering regimes. Geochim. Cosmochim. Acta 164, 71–93.

Dessert, C., Lajeunesse, E., Lloret, E., Clergue, C., Crispi, O., Gorge, C., Quidelleur, X., 2015. Controls on chemical weathering on a mountainous volcanic tropical island: Guadeloupe (French West Indies). Geochim. Cosmochim. Acta 171, 216–237.

Dessert, C., Clergue, C., Rousteau, A., Crispi, O., Benedetti, M.F., 2020. Atmospheric contribution to cations cycling in highly weathered catchment, Guadeloupe (Lesser Antilles). Chem. Geol. 531, 119354.

Favier, A., Lardeaux, J.-M., Legendre, L., Verati, C., Philippon, M., Corsini, M., Münch, P., Ventalon, S., 2019. Tectonometamorphic evolution of shallow crustal levels within active volcanic arcs. Insights from the exhumed Basal Complex of Basse-Terre (Guadeloupe, French West Indies), BSGF - Earth Sciences Bulletin 190: 10.

Fernandez, N.M., Bouchez, J., Derry, L.A., Chorover, J., Gaillardet, J., Giesbrecht, I., Fries, D., Druhan, J.L., 2022. Resiliency of silica export signatures when low order streams are subject to storm events. J. Geophys. Res. Biogeo. 127.

Flesch, G., Anderson Jr., A., Svec, H., 1973. A secondary isotopic standard for 6Li/7Li determinations. Int. J. Mass Spectrom. Ion Phys. 12 (3), 265–272.

Fouillac, Ch., Michard, G., 1981. Sodium/lithium ratio in water applied to geothermometry of geothermal reservoirs. Geothermics 10, 55–70.

Franzson, H., Zierenberg, R., Schiffman, P., 2008. Chemical transport in geothermal systems in Iceland. evidence from hydrothermal alteration. J. Volcanol. Geoth. Res. 173, 217–229.

Fries, D.M., James, R.H., Dessert, C., Bouchez, J., Beaumais, A., Pearce, C.R., 2019. The response of Li and Mg isotopes to rain events in a highly-weathered catchment. Chem. Geol. 519, 68–82.

Gaillardet, J., Rad, S., Rivé, K., Louvat, P., Gorge, C., Allègre, C.-J., Lajeunesse, E., 2011. Orography-driven chemical denudation in the Lesser Antilles: evidence for a new feed-back mechanism stabilizing atmospheric CO2. Am. J. Sci. 311, 851–894.

Gaillardet, J., Braud, I., Hankard, F., et al., 2018. OZCAR: the French network of critical zone observatories. Vadose Zone J. 17.

Gaspard, F., Opfergelt, S., Dessert, C., Robert, V., Ameijeir, Y., Delmelle, P., 2021. Imprint of chemical weathering and hydrothermalism on the Ge/Si ratio and Si isotopic composition of rivers in a volcanic tropical island. Chem. Geol, Basse-Terre, Guadeloupe (French West Indies).

Goddéris, Y., François, L.M., 1995. The Cenozoic evolution of the strontium and carbon cycles: relative importance of continental erosion and mantle exchanges. Chem. Geol. 126, 169–190.

Golla, J.K., Bouchez, J., Kuessner, M.L., Rempe, D.M., Druhan, J.L., 2022. Subsurface weathering signatures in stream chemistry during an intense storm. Earth Planet. Sci. Lett. 595, 117773.

Guérin, A., Devauchelle, O., Robert, V., Kitou, T., Dessert, C., Quiquerez, A., Allemand, P., Lajeunesse, E., 2019. Stream discharge surges generated by groundwater flow. Geophys. Res. Lett.

Guo, J., Maa, L., Gaillardet, J., Sak, P.B., Pereyra, Y., Engel, J., 2020. Reconciling chemical weathering rates across scales: Application of uranium-series isotope systematics in volcanic weathering clasts from Basse-Terre Island (French Guadeloupe). Earth Planet. Sci. Lett. 530, 115874.

Henchiri, S., Clergue, C., Dellinger, M., Gaillardet, J., Louvat, P., Bouchez, J., 2014. The influence of hydrothermal activity on the Li isotopic signature of rivers draining volcanic areas. Proc. Earth Planet. Sci. 10, 223–230.

Henchiri, S., Gaillardet, J., Dellinger, M., Bouchez, J., Spencer, R.G.M., 2016. Riverine dissolved lithium isotopic signatures in low-relief central Africa and their link to weathering regimes. Geophys. Res. Lett. 43.

Henriet, C., De Jaeger, N., Dorel, M., Opfergelt, S., Delvaux, B., 2008. The reserve of weatherable primary silicates impacts the accumulation of biogenic silicon in volcanic ash soils. Biogeochemistry 90, 209–223.

Hindshaw, R.S., Tosca, R., Goût, T.L., Farnan, I., Tosca, N.J., Tipper, E.T., 2019. Experimental constraints on Li isotope fractionation during clay formation. Geochim. Cosmochim. Acta 250, 219–237.

Huh, Y., Chan, L., Zhang, L., Edmond, J., 1998. Lithium and its isotopes in major world rivers: implications for weathering and the oceanic budget. Geochim. Cosmochim. Acta 62 (12), 2039–2051.

Huh, Y., Chan, L., Edmond, J., 2001. Lithium isotopes as a probe of weathering processes: Orinoco River. Earth Planet. Sci. Lett. 194 (1–2), 189–199.

Kharaka, Y.K., Lico, M.S., Law, L.M., 1982. Chemical geothermometers applied to formation waters, Gulf of Mexico and California Basins (abstract). Am. Ass. Petrol. Geol. Bull. 66, 588.

Kisakurek, B., James, R., Harris, N., 2005. Li and δ7Li in Himalayan Rivers: proxies for silicate weathering? Earth Planet. Sci. Lett. 237 (3–4), 387–401.

Komorowski, J.K., Boudon, G., Semet, M., Beauducel, F., Anténor-Habazac, C., Bazin, S., Hammouya, G., Lindsay, J., Robertson, R., Shepherd, J., et al., 2005. Volcanic hazard atlas of the Lesser Antilles. by J. Lindsay et al, 65–102.

Lemarchand, E., Chabaux, F., Vigier, N., Millot, R., Pierret, M., 2010. Lithium isotope systematics in a forested granitic catchment (Strengbach, Vosges Mountains, France). Geochim. Cosmochim. Acta 74 (16), 4612–4628.

Li, W., Liu, X.M., 2020. Experimental investigation of lithium isotope fractionation during kaolinite adsorption: Implications for chemical weathering. Geochim. Cosmochim. Acta 284, 156–172.

Li, L., Bonifacie, M., Aubaud, C., Crispi, O., Dessert, C., Agrinier, P., 2015. Chlorine isotopes of thermal springsin arc volcanoes for tracing shallow magmatic activity. Earth Planet. Sci. Lett. 413, 101–110.

Li, G., West, A.J., 2014. Evolution of Cenozoic seawater lithium isotopes: coupling of global denudation regime and shifting seawater sinks. Earth Planet. Sci. Lett. 401, 284–293.

Liu, X.M., Wanner, C., Rudnick, R.L., McDonough, W.F., 2015. Processes controlling δ^7Li in rivers illuminated by study of streams and groundwaters draining basalts. Earth Planet. Sci. Lett. 409, 212–224.

Lloret, E., Dessert, C., Gaillardet, J., Albéric, P., Crispi, O., Chaduteau, C., et al., 2011. Comparison of dissolved inorganic and organic carbon yields and fluxes in the watersheds of tropical volcanic islands, examples from Guadeloupe (French West Indies). Chem. Geol. 280, 65–78.

Lloret, E., Dessert, C., Pastor, L., Lajeunesse, E., Crispi, O., Gaillardet, J., Benedetti, M.F., 2013. Dynamic of particulate and dissolved organic carbon in small volcanic mountainous tropical watersheds. Chem. Geol. 351, 229–244.

Lloret, E., Dessert, C., Buss, H.L., Chaduteau, C., Huon, S., Alberic, P., Benedetti, M.F., 2016. Sources of dissolved organic carbon in small volcanic mountainous tropical rivers, examples from Guadeloupe (French West Indies). Geoderma 282, 129–138.

Louvat, P., Gislason, S.R., Allègre, C.J., 2008. Chemical and mechanical erosion rates in Iceland as deduced from river dissolved and solid material. Am. J. Sci. 308, 679–726.

Louvat, P., Gaillardet, J., Paris, G., Dessert, C., 2011. Boron isotope ratios of surface waters in Guadeloupe, Lesser Antilles. Appl. Geochem. 26, S76–S79.

Metcalfe, A., Moune, S., Komorowski, J.C., Moretti, R., 2022. Bottom-up vs topdown drivers of eruption style: Petro-geochemical constraints from the Holocene explosive activity at La Soufrière de Guadeloupe. J. Volcanol. Geoth. Res. 424, 107488.

Millot, R., Girard, J., 2007. Lithium isotope fractionation during adsorption onto mineral surfaces. International Meeting on Clays in Natural & Engineered Barriers for Radioactive Waste Confinement, Lille, France 307–308. http://www.andra.fr/lille2007/abstract_lille2007/donnees/pdf/307_308_P_GM_6.pdf.

Millot, R., Scaillet, B., Sanjuan, B., 2010. Lithium isotopes in island arc geothermal systems: Guadeloupe, Martinique (French West Indies) and experimental approach. Geochim. Cosmochim. Acta 74 (6), 1852–1871.

Millot, R., Vigier, N., Gaillardet, J., 2010. Behaviour of lithium and its isotopes during weathering in the Mackenzie Basin. Canada. Geochim. Cosmochim. Acta 74 (14), 3897–3912.
Millot, R., Hegan, A., Négrel, P., 2012. Geothermal waters from the Taupo Volcanic Zone, New Zealand: Li, B and Sr isotopes characterization. Appl. Geochem. 27, 677–688.
Misra, S., Froelich, P., 2012. Lithium isotope history of Cenozoic seawater: changes in silicate weathering and reverse weathering. Science 335 (6070), 818–823.
Murphy, M.J., Porcelli, D., Pogge von Strandmann, P.A.E., Hirst, C.A., Kutscher, L., Katchinoff, J.A., Mörth, C.M., Maximov, T., Andersson, P.S., 2019. Tracing silicate weathering processes in the permafrost-dominated Lena River watershed using lithium isotopes. Geochim. Cosmochim. Acta 245, 154–171.
Navelot, V., Géraud, Y., Favier, A., Diraison, M., Corsini, M., Lardeaux, J.M., et al., 2018. Petrophysical properties of volcanic rocks and impacts of hydrothermal alteration in the Guadeloupe Archipelago (West Indies). J. Volcanol. Geoth. Res. 360, 1–21.
Parat, F., Dungan, M.A., Streck, M.J., 2002. Anhydrite, pyrrhotite, and sulfur-rich apatite: tracing the sulfur evolution of an Oligocene andesite (Eagle Mountain, CO, USA). Lithos 64, 63–75.
Patrier, P., Bruzac, S., Pays, R., Beaufort, D., Bouchot, V., Verati, C., Gadalia, A., 2013. Occurrence of epithermal breccias in the Bouillante geothermal field (Basse Terre – Guadeloupe). Bulletin De La Société Géologique De France 184, 119–128.
Pasquet, S., Marçais, J., Hayes, J.L., Sak, P.B., Ma, L., Gaillardet, J., 2022. Catchment scale architecture of the deep critical zone revealed by seismic imaging. Geophys. Res. Lett. 49 (13), e2022GL098433.
Pistiner, J.S., Henderson, G.M., 2003. Lithium isotope fractionation during continental weathering processes. Earth Planet. Sci. Lett. 214, 327–339.
Pogge von Strandmann, P.A.E., Burton, K.W., James, R.H., van Calsteren, P., Gislason, S. R., Mokadem, F., 2006. Riverine behaviour of uranium and lithium isotopes in an actively glaciated basaltic terrain. Earth Planet. Sci. Lett. 251, 134–147.
Pogge von Strandmann, P.A.E., Burton, K.W., James, R.H., van Calsteren, P., Gislason, S. R., 2010. Assessing the role of climate on uranium and lithium isotope behavior in rivers draining a basaltic terrain. Chem. Geol. 270 (1), 227–239.
Pogge von Strandmann, P.A.E., Burton, K.W., Opfergelt, S., Eiríksdóttir, E.S., Murphy, M. J., Einarsson, A., Gislason, S.R., 2016. The effect of hydrothermal spring weathering processes and primary productivity on lithium isotopes: Lake Myvatn. Iceland. Chem. Geol. 445, 4–13.
Pogge von Strandmann, P.A.E., Fraser, W.T., Hammond, S.J., Tarbuck, G., Wood, I.G., Oelkers, E.H., Murphy, M.J., 2019. Experimental determination of Li isotope behaviour during basalt weathering. Chem. Geol. 517, 34–43.
Pogge von Strandmann, P.A.E., Burton, K.W., Opfergelt, S., Genson, B., Guicharnaud, R. A., Gislason, S.R., 2021. The lithium isotope response to the variable weathering of soils in Iceland. Geochim. Cosmochim. Acta 313, 55–173.
Pogge von Strandmann, P.A.P., Cosford, L.R., Liu, C.Y., Liu, X., Krause, A.J., Wilson, D.J., Burton, K.W., 2023. Assessing hydrological controls on the lithium isotope weathering tracer. Chem. Geol. 642, 121801.
Rad, S., Louvat, P., Gorge, C., Gaillardet, J., Allègre, C.J., 2006. River dissolved and solid loads in the Lesser Antilles: new insight into basalt weathering processes. J. Geochem. Explor. 88, 308–312.
Rad, S., Rivé, K., Vittecoq, B., Cerdan, O., Allègre, C.J., 2013. Chemical weathering and erosion rates in the Lesser Antilles: an overview in Guadeloupe, Martinique and Dominica. J. S. Am. Earth Sci. 45, 331–344.
Raymo, M.E., Ruddiman, W.F., 1992. Tectonic forcing of late Cenozoic climate. Nature 359 (6391), 117–122.
Ricci, J., Quidelleur, X., Pallares, C., Lahitte, P., 2017. High-resolution K-Ar dating of a complex magmatic system: the example of Basse-Terre Island (French West Indies). J. Volcanol. Geoth. Res. 345, 142–160.
Rivé, K., Gaillardet, J., Agrinier, P., Rad, S., 2013. Carbon isotopes in the rivers from the Lesser Antilles: origin of the carbonic acid consumed by weathering reactions in the Lesser Antilles. Earth Surf. Proc. Land. 38, 1020–1035.
Rosas-Carbajal, M., Komorowski, J.-C., Nicollin, F., Gibert, D., 2016. Volcano electrical tomography unveils edifice collapse hazard linked to hydrothermal system structure and dynamics. Sci. Rep. 6 (1), 29899.
Rugenstein, J.K.C., Ibarra, D.E., von Blanckenburg, F., 2019. Neogene cooling driven by land surface reactivity rather than increased weathering fluxes. Nature 571 (7763), 99–102.
Ruzié, L., Aubaud, C., Moreira, M., Agrinier, P., Dessert, C., Gréau, C., Crispi, O., 2013. Carbon and helium isotopes in thermal springs of La Soufrière volcano (Guadeloupe, Lesser Antilles): Implications for volcanological monitoring. Chem. Geol. 359, 70–80.
Ryu, J.-S., Vigier, N., Lee, S.-W., Lee, K.-S., Chadwick, O.A., 2014. Variation of lithium isotope geochemistry during basalt weathering and secondary mineral transformations in Hawaii. Geochim. Cosmochim. Acta 145, 103–115.
Sak, P.B., Navarre-Stichler, A.K., Miller, C.E., Daniel, C.C., Gaillardet, J., Buss, H.L., Lebedeva, M.I., Brantley, S.L., 2010. Controls on rind thickness on basaltic andesite clasts weathering in Guadeloupe. Chem. Geol. 276, 129–143.
Salaün, A., Villemant, B., Gerard, M., Komorowski, J.-C., Agnes, M., 2011. Hydrothermal alteration in andesitic volcanoes: trace element redistribution in active and ancient hydrothermal systems of Guadeloupe (Lesser Antilles). Fuel. Energ. Abstr. 111, 59–83.
Samper, A., Quidelleur, X., Lahitten, P., Mollex, D., 2007. Timing of effusive volcanism and collapse events within an oceanic arc island: Basse-Terre, Guadeloupe archipelago (Lesser Antilles Arc). Earth Planet. Sci. Lett. 258, 175–191.
Samper, A., Quidelleur, X., Komorowski, J.-C., Lahitte, P., Boudon, G., 2009. Effusive history of the Grande Découverte Volcanic complex, southern Basse-Terre (Guadeloupe, French West Indies) from new K–Ar Cassignol–Gillot ages. J. Volcanol. Geoth. Res. 187, 117–130.
Sanjuan, B., Millot, R., Ásmundsson, R., Brach, M., Giroud, N., 2014. Use of two new Na/Li geothermometric relationships for geothermal fluids in volcanic environments. Chem. Geol. 389, 60–81.
Sawhney, B., 1972. Selective sorption and fixation of cations by clay minerals: a review. Clays Clay Miner. 20, 93–100.
Tamburello, G., Moune, S., Allard, P., Venugopal, S., Robert, V., Rosas-Carbajal, M., Deroussi, S., Kitou, G., Didier, T., Komorowski, J.C., Beauducel, F., de Chabalier, J. B., LeMarchand, A., Le Friant, A., Bonifacie, M., Dessert, C., Moretti, R., 2019. Spatio-Temporal Relationships between Fumarolic activity, Hydrothermal Fluid Circulation and Geophysical Signals at an Arc Volcano in Degassing Unrest: La Soufrière of Guadeloupe (French West Indies). Geosciences 9, 480.
Vander Linden, C., Li, Z., Iserentant, A., Van Ranst, E., de Tombeur, F., Delvaux, B., 2021. Rainfall is the major driver of plant Si availability in perudic gibbsitic Andosols. Geoderma 404, 115295.
Van Laere, G., Gall, Y., Rousteau, A., 2016. The Forest Ecosystems Observatory in Guadeloupe (FWI). Caribbean Naturalist, Special Issue N°1, 108–115.
Verati, C., Patrier-Mas, P., Lardeaux, J.-M., Bouchot, V., 2014. Timing of geothermal activity in an active island-arc volcanic setting: first 40Ar/39Ar dating from Bouillante geothermal field (Guadeloupe, French West Indies). Geol. Soc. Lond. Spec. Publ. 378, 285–295.
Verney-Carron, A., Vigier, N., Millot, R., 2011. Experimental determination of the role of diffusion on Li isotope fractionation during basaltic glass weathering. Geochim. Cosmochim. Acta 75, 3452–3468.
Verney-Carron, A., Vigier, N., Millot, R., Hardarson, B.S., 2015. Lithium isotopes in hydrothermally altered basalts from Hengill (SW Iceland). Earth Planet. Sci. Lett. 411, 62–71.
Vigier, N., Decarreau, A., Millot, R., Carignan, J., Petit, S., France-Lanord, C., 2008. Quantifying Li isotope fractionation during smectite formation and implications for the Li cycle. Geochim. Cosmochim. Acta 72 (3), 780–792.
Vigier, N., Gislason, S., Burton, K., Millot, R., Mokadem, F., 2009. The relationship between riverine lithium isotope composition and silicate weathering rates in Iceland. Earth Planet. Sci. Lett. 287 (3), 434–441.
Vigier, N., Goddéris, Y., 2015. A new approach for modeling Cenozoic oceanic lithium isotope paleo-variations: the key role of climate. Clim. Past 11 (4), 635–645.
Villemant, B., Komorowski, J.-C., Dessert, C., Michel, A., Crispi, O., Hammouya, G., Beauducel, F., de Chabalier, J.-B., 2014. Evidence for a new shallow magma intrusion at La Soufrière of Guadeloupe (Lesser Antilles), Insights from long-term geochemical monitoring of halogen-rich hydrothermal fluids. J. Volcanol. Geoth. Res. 285, 247–277.
Walker, J., Hays, P., Kasting, J., 1981. A negative feedback mechanism for the long-term stabilization of the Earth's surface temperature. J. Geophys. Res. 86 (C10), 9776–9782.
Wang, Q.L., Chetelat, B., Zhao, Z.Q., Ding, H., Li, S.L., Wang, B.L., Liu, X.L., 2015. Behavior of lithium isotopes in the Changjiang River system: sources effects and response to weathering and erosion. Geochim. Cosmochim. Acta 151, 117–132.
Westercamp, D., 1988. Magma generation in the Lesser Antilles: geological constraints. Tectonophysics 149, 145–163.
Williams, L.B., Hervig, R.L., 2005. Lithium and boron isotopes in illite–smectite: the importance of crystal size. Geochim. Cosmochim. Acta 69, 5705–5716.
Wimpenny, J., Gislason, S.R., James, R.H., Gannoun, A., Pogge Von Strandmann, P.A.E., Burton, K.W., 2010. The behaviour of Li and Mg isotopes during primary phase dissolution and secondary mineral formation in basalt. Geochim. Cosmochim. Acta 74, 5259–5279.
Winnick, M.J., Druhan, J.L., Maher, K., 2022. Weathering intensity and lithium isotopes: a reactive transport perspective. Am. J. Sci. 322 (5), 647–682.
Xu-Yang, Y., Dessert, C., Losno, R., 2022. Atmospheric deposition over the Caribbean region: Sea salt and Saharan dust are sources of essential elements on the island of Guadeloupe. J. Geophys. Res. Atmos. 127, e2022JD037175.
Xu-Yang, Y., Losno, R., Dessert, C., Monna, F., Mahowald, N.M., Tharaud, M., 2025. Atmospheric aerosols versus total atmospheric deposition in Guadeloupe (Lesser Antilles): Composition, concentration, and flux. J. Geophys. Res. Atmos. 130, e2024JD042682.
Zhang, F., Dellinger, M., Hilton, R.G., Yu, J., Allen, M.B., Densmore, A.L., Sun, H., Jin, Z., 2022. Hydrological control of river and seawater lithium isotopes. Nat. Commun. 13 (1), 3359.
Zhang, J.-W., Yan, Y.-N., Zhao, Z.-Q., Liu, X.-M., Li, X.-D., Zhang, D., Ding, H., Meng, J.-L., Liu, C.-Q., 2022. Spatiotemporal variation of Li isotopes in the Yarlung Tsangpo River basin (upper reaches of the Brahmaputra River): source and process. Earth and Planetary Science Letters 600.